HHS Public Access

Author manuscript

ACS Appl Bio Mater. Author manuscript; available in PMC 2022 November 16.

Published in final edited form as:

ACS Appl Bio Mater. 2022 June 20; 5(6): 2643–2663. doi:10.1021/acsabm.2c00109.

Mass Spectrometry, Structural Analysis and Anti-Inflammatory Properties of Photocrosslinked Human Albumin Hydrogels

Shahriar Sharifi[1], **Amir Ata Saei**[2,3], **Hassan Gharibi**[2], **Nouf N Mahmoud**[4], **Shannon Harkins**[1], **Naruphorn Dararatana**[1], **Erika M Lisabeth**[5], **Vahid Serpooshan**[6,7,8], **Ákos Végvári**[2,9], **Anna Moore**[1,*], **Morteza Mahmoudi**[1,*]

[1]Department of Radiology and Precision Health Program, Michigan State University, East Lansing, MI, 48824, United States

[2]Division of Physiological Chemistry I, Department of Medical Biochemistry and Biophysics, Karolinska Institutet, SE-17 177 Stockholm, Sweden

[3]Department of Cell Biology, Harvard Medical School, Boston, MA 02115, USA

[4]Faculty of Pharmacy, Al-Zaytoonah University of Jordan, Amman 11733, Jordan.

[5]Department of Pharmacology and Toxicology, Michigan State University, East Lansing, MI, 48824, United States and Biophysics, Karolinska Institute, SE-17 177 Stockholm, Sweden

[6]Department of Biomedical Engineering, Emory University School of Medicine and Georgia Institute of Technology, Atlanta, GA 30322, USA

[7]Department of Pediatrics, Emory University School of Medicine, Atlanta, GA 30322, USA

[8]Children's Healthcare of Atlanta, Atlanta, GA 30322, USA

[9]Proteomics Biomedicum, Division of Physiological Chemistry I, Department of Medical Biochemistry

Abstract

Protein-based hydrogels are at the forefront of biomaterials research mainly due to their superb inherent biological functionalities. Among them, albumin-based hydrogels offer unique benefits such as non-immunogenicity, biodegradability, and high binding affinity to various biomolecules, which make them suitable candidate for drug delivery systems or biomedical applications. Amongst various methods for preparation of albumin hydrogels, modification of albumin with methacrylic anhydride (MAA) is a facile method to introduce polymerizable groups with minimum alteration in the protein structure or denaturation. Here we report a photocurable human serum-based hydrogel synthesized by methacryloylation of human serum albumin by MAA. Given the presence of 585 amino acids in human serum albumin (HSA), with five

*Corresponding authors; (AM): moorea57@msu.edu (MM): mahmou22@msu.edu.

Supplementary information. Full details of the Materials and Methods.

Competing interests

Morteza Mahmoudi discloses that (i) he is a co-founder and director of the Academic Parity Movement (www.paritymovement.org), a non-profit organization dedicated to addressing academic discrimination, violence and incivility; (ii) he is a Founding Partner at Partners in Global Wound Care (PGWC); and (iii) he receives royalties/honoraria for his published books, plenary lectures, and licensed patent. The author declares no conflicts of interest.

nucleophilic amino acids capable of reacting with acid anhydrides, we used matrix-assisted laser desorption ionization-time of flight mass spectrometry and liquid chromatography-tandem mass spectrometry to evaluate the extent of modification and to identify the amino acids reacting with MAA. Size exclusion chromatography examined the effect of methacryloylation and ultraviolet light irradiation on enzymatic and hydrolytic degradation of methacrylated albumin macromer and its crosslinked hydrogels. Moreover, the impacts of methacryloylation and crosslinking on alteration of albumin biological function (inflammatory response and toxicity) were evaluated *in vitro* using brain-derived HMC3 macrophages. Results revealed that the lysines in HSA were the primary targets reacting with MAA. Modification of other amino acids, such as cysteine, threonine, serine, and tyrosine, with MAA was also confirmed. The methacrylated HSA and its derived hydrogels were non-toxic and did not induce inflammatory pathways, while significantly reducing macrophage adhesion to the hydrogels (one the key steps in the process of foreign body reaction to biomaterials). Of note, the albumin-based hydrogels demonstrated anti-inflammatory response modulating cellular events in HMC3 macrophages. The biocompatibility and angiogenic response to methacrylated HSA and resulting hydrogels was further evaluated using an ex ovo chick chorioallantoic membrane assay, which confirmed biocompatibility with chicken embryos along with slight angiogenesis-modulating effects.

Introduction

Hydrogels have been extensively explored for various biomedical applications including tissue engineering scaffolds, drug delivery systems, and medical devices. Due to their biocompatibility, ability to hold high water content, and wide range of physicochemical properties, hydrogels can function as a biomimetic platform to reproduce *in vivo* microenvironment features such as extracellular matrix (ECM)[1]. Hydrogels can also support other essential biological features (e.g., facilitation of transport of nutrients and waste through their interconnected pore architecture) while facilitating design or functionalization to introduce bioactivity or smart features responding to external stimuli[2–3]. Although various types of synthetic hydrogels have been developed to mimic the physicochemical and mechanical properties of natural tissues, their lack of robust cell adhesion properties has limited their safe and efficient application in tissue engineering and regenerative medicine[4–5]. In contrast, natural hydrogels, which are often based on proteins, polysaccharides, or a mixture of both, or are derived from decellularized tissue, have frequently been used for various biomedical applications due to their inherent biocompatibility, bioactivity, and biodegradability[6].

Currently, many natural proteins (e.g., fibrin, collagen, gelatin, silk, tropoelastin, and albumin) have been used for natural hydrogel preparation[6]. Human serum albumin (HSA) is a highly water-soluble small globular protein made of a single chain of 585 amino acids, has a molecular weight of 66,348 Da, and is the most abundant protein in blood, with an average half-life of 19 days[7]. Produced by hepatocytes with a concentration of around 35–50 g/L in blood, this non-glycosylated endogenous protein plays a major role in the maintenance of both intravascular and extravascular colloid osmotic pressure[8–9]. HSA is a well-known material for drug therapy with a long history of medical applications[10–13]. As a versatile carrier protein with multiple ligand binding sites for various endogenous

and exogenous molecules, it has mainly been used as i) a carrier molecule for numerous compounds such as fatty acids, metals, or drugs in drug delivery or controlled release systems; or ii) a surgical adhesive/sealant[14–16]. Although many studies have explored the potential of albumin as a molecular drug carrier, its use as a hydrogel in biomedical research has received far less attention. Nonetheless, since albumin hydrogels offer unique features such as biodegradability, non-immunogenicity, and biocompatibility, as well as the ability to bind to various biomolecules, interest is steadily growing. For example, recent studies have explored the application of albumin hydrogels as a biomaterial for implants or three-dimensional (3D) scaffolds for several tissue engineering applications including cardiac, orthopedic, and neural tissue regeneration[17–21].

Chemical crosslinking is the most common method for synthesizing albumin-based hydrogels,[22] though physical methods are also used. Additions of multifunctional crosslinkers molecules containing amine-reactive groups (e.g., genipin and glutaraldehyde), disulfide crosslinkers, or thiol-reactive groups to pristine albumin or its thiolated derivative results in the formation of a 3D albumin network[23–27]. Physical crosslinking approaches are mainly based on pH-induced crosslinking and thermal crosslinking. Albumin is a globular protein, and although it has good resistance to thermal denaturation, heating eventually causes conformational changes, which ultimately leads to the creation of network structures by aggregation of heat-denatured albumin[28–30]. Similarly, acidic or basic pH also causes conformational isomeric changes in the albumin molecule, resulting in self-assembly into a hydrogel network by hydrophobic interactions and counterion binding mechanisms[17, 29, 31–32]. However, the resulting hydrogels are not ideal for medical applications, as the crosslinking agents or non-neutral pH conditions are often toxic to cells and require extraction or neutralization, limiting cell encapsulations or other biomedical applications. Albumin is known to attach to a number of proteins and receptors in various tissues and cell lines, such as Albondin/gp60, SPARC, and FcRn[7]. However, physical (and often chemical) crosslinking not only alters the secondary and tertiary native heart-shaped globular conformation of albumin but may also change their active site, altering binding affinities or even inducing immunogenicity.

Alternatively, albumin hydrogels can be prepared using a photocrosslinking reaction. This approach utilizes ultraviolet light or visible light in the presence of photoinitiators and mildly modified albumin, introducing a photoreactive moiety in the albumin chain, producing three-dimensional hydrogels with controlled spatial resolution, size, and shape. The methacryloylation of albumin using methacrylic anhydride or glycidyl methacrylate in controlled pH is the most common approach for functionalization of albumin or other biomacromolecules[33–34]. Spectrophotometric studies (e.g., circular dichroism and attenuated total reflectance-Fourier transform infrared) have shown that this only mildly alters the secondary structure of albumin. For example, it was demonstrated that the fractional helicity of bovine serum albumin (BSA) after 100% methacryloylation was reduced only by about 6% compared to native BSA. The secondary structure of the fully methacryloylated albumin was also largely maintained, as only mild changes in α-helix and β-turn values were observed[35]. These results have been corroborated by other studies, which confirmed that methacryloylation does not change the secondary structure of BSA[36]. Interestingly, an enzymatic study using para-nitrophenyl acetate as the substrate also demonstrated that

the enzyme-like activity of the methacrylated albumin hydrogel was partially retained, indicating neither methacryloylation nor network formation significantly alter the structure of albumin[37].

BSA and HSA differ by <1% in molecular weight and have a similar isoelectric point; nevertheless, they share only 76% sequence identity[38]. Due to these structural and sequence similarities, the majority of the albumin-based hydrogels in the literature are made using BSA, leaving HSA hydrogels relatively understudied. To our knowledge, very few studies have investigated the properties of non-denatured or minimally denatured albumin hydrogels made from HSA. Table S1 of the Supplementary Information (SI) summarizes the primary research conducted on albumin hydrogels for various biomedical application.

Here we investigated a photocurable albumin hydrogel made from HSA methacrylate. HSA methacrylate macromers were synthesized using methacrylic anhydride, followed by crosslinking of the macromers in the presence of water-soluble and biocompatible initiator lithium phenyl-2,4,6-trimethylbenzoylphosphinate (LAP). While this chemistry is widely used in the methacryloylation of both synthetic polymers and proteins, there has been no in-depth investigation of the details of this reaction at the amino-acid level for HSA. The extent and specificity of this reaction is critical in the toxicity, bioavailability, and immunomodulatory capability of protein-based macromers. For example, methacrylic anhydride can react with amino acids containing amine, hydroxyl, or thiol groups, resulting in the formation of methacrylamide, methacrylate, or thioester functionality, respectively. Such modification may alter the protein structure. Since distinguishing chemical shifts in these functionalities in the NMR spectrum of HSA is challenging, we used liquid chromatography-mass spectrometry (LC-MS/MS) and enzymatic digestion to identify the amino acid residues in HSA, which reacts with methacrylic anhydride under our reaction conditions. In addition to molecular characterization, hydrogel characteristics (e.g., swelling, enzymatic and hydrolytic degradation, pore structure and size) were analyzed using a wide range of techniques including a swelling study, size exclusion chromatography, and scanning electron microscopy (SEM).

The passivation effect of albumin coatings and its effects on suppression of immune cell attachment to the surface of biomaterials have long been established[39–41]. However, to our knowledge, there is no study of photocrosslinked HSA hydrogels and their possible immunomodulatory potential using immune cells. We hypothesized that albumin hydrogels could modulate protein absorption, affecting cell adhesion and consequently influencing the immune reaction to the biomaterial. Hence, we used the brain-derived human microglial (macrophage) cell line HMC3 to evaluate the toxicity, cell attachment, proliferation, and inflammatory response of both HSA methacrylate (HSAMA) and resulting hydrogels. Human microglia are of particular interest, as they are activated upon injury to the brain vasculature and are the major cell type regulating the neuroinflammatory response to implanted biomaterial in the brain, such as intracortical microelectrodes[42]. Furthermore, the biocompatibility of HSAMA and HSAMA-containing hydrogels and their impact on blood vessel development were explored using a chicken embryo model. This alternative to rodent models is an inexpensive, rapid, highly reproducible, and easy-to-handle model with a lower potential for pain perception[43]. The chick embryo chorioallantoic membrane (CAM)

is the thin, transparent outermost extraembryonic membrane and is highly vascularized for nutrient and gas exchange. CAM development begins on embryonic day four. The chicken embryo model shows similar patterns of cellular toxicity as *in vitro* models and gives tissue responses similar to those in mammalian models; thus, it is widely used in toxicity studies and wound healing research. This model also facilitates the study of the biological and toxicological responses to a broad range of materials without species-specific restrictions, due to its immature immune system[44–45].

This report will outline the development of anti-inflammatory photocrosslinked albumin hydrogels for tissue engineering applications (e.g., wound healing and low inflammatory coatings for implants).

Results and discussion

HSA methacryloyl was synthesized by reacting HSA with excess methacrylic anhydride in the presence of sodium hydroxide (Figure 1). The resulting methacrylic acid quickly reduces the pH of the solution. Therefore, to minimize the possibility of protonation of amino groups in lysine residues at an acidic pH, and considering the tendency of proteins to denature, aggregate, and precipitate at their isoelectric point (pI = 4.7 of HSA), concentrated sodium hydroxide solution was added to keep the pH of the reaction neutral[46]. Overnight incubation at 4°C then resulted in the crystallization of methacrylic acid and salt, which allowed facile removal of the bulk of low water-soluble impurities before the dialysis step, yielding a cleaner product. The degree of methacrylation (DM) of albumin methacryloyl is a critical factor determining the physical, chemical, and biological properties of the hydrogels. To measure the DM value, we used 2,4,6-Trinitrobenzene Sulfonic Acid (TNBS) assay, which confirmed 100% substitution of the amino group in lysine residues with methacrylamide groups. This is consistent with previous studies, which showed that reacting BSA lysine residues with 3–5 molar excess of MAA results in 100% functionalization of BSA[47]. Although the substitution appears quantitative, the TNBS assay showed that pure HSA had only 30 available amino groups in lysine residues, while 59 lysine residues were present in the HSA sequence. This result is consistent with other studies demonstrating that only half of theoretical lysine residues in BSA were reacted and were identifiable by TNBS assay[35]. This finding is probably related to the globular nature of HSA (and BSA), which affects lysine reactivity. In fact, since some of the lysine residues (n=12) are buried inside the protein interior, they are not readily accessible to react with TNBS in an aqueous environment[48]. This is corroborated by the fact that other studies have also indicated that 30–35 or more of 59 of lysine residues are available for chemical modification[49–50].

To further investigate the nature of the methacryloylation reaction, the molecular weights of HSA and HSAMA were analyzed by matrix-assisted laser desorption ionization-time of flight mass spectrometry (MALDI-TOF-MS; Figure S1 of the SI). The molecular weight of HSA was increased by about 4,535 Da by modification with MAA, reaching 71,211 Da. Assuming that lysine moieties are the primary amino acids reacting with MAA, it can be concluded that 54 −56 lysines (and/or other residues) are methacrylated under the reaction conditions. This finding, however, is contrary to an early assumption that about 20% of lysine residues are buried and not solvent-accessible to react with MAA[51].

This discrepancy can be addressed by two hypotheses: 1) the majority of the lysine residues have been reacted under our conditions or 2) methacryloylation is not limited to lysine residues. In fact, in addition to Lys, there are four other amino acids in HSA with nucleophilic chemical groups that could also potentially react with MAA, *i.e.,* -SH group of cysteine and -OH groups of serine, tyrosine, and threonine (Figure 1). In addition, the resulting HSAMA also had much greater polydispersity than HSA, as shown in MALDI-TOF-MS spectra, suggesting that lysine (and/or possibly other amino acids) are not equally reacting with MAA in every HSA molecule. This difference in molecular weight distribution of HSAMA can affect the physicochemical properties of the resulting hydrogel.

To further validate the finding that more lysine residues or other amino acids are also involved in the reaction, we acquired LC-MS/MS spectra of both HSA and two separately synthesized HSAMA batches to capture the distribution of methacrylate groups on HSAMA among various amino acid residues (Figure S1 of the SI). We used the optimal enzymes for HSA digestion, the combination of which, when used separately, would give the highest sequence coverage in LC-MS/MS. Following optimized procedures, HSA and HSAMA were proteolytically cleaved with trypsin and GluC independently to release a library of shorter oligopeptides, which were separated by chromatography and measured by tandem MS. Trypsin cleaves proteins on the C-terminal side of Lys and Arg residues. Since methacryloylation reaction mainly targets Lys, it is highly plausible that the HSAMAs have lower susceptibility than HSA to trypsin. Hence samples were also treated with GluC, which preferentially cleaves peptide bonds at C-terminal to Glu and at lower rate to Asp residues.

The Mascot search algorithm coupled with Proteome Discoverer were used to identify the digested peptide sequences and monitor the sequence coverage provided. Three different peptide searches were performed with and without the modifications, using the following criteria: i) with acetylation at N-termini, carbamidomethylation on Cys, deamidation on Asn and Gln, and oxidation on Met. This search would show the sequence coverage of unmodified HSA as a quality control; ii) methacryloylation on Lys, acetylation at N-termini, carbamidomethylation on Cys, deamidation on Asn and Gln, and oxidation on Met; and iii) methacryloylation on Lys, Cys, Ser, Thr, Tyr, acetylation at N-termini, carbamidomethylation on Cys, deamidation on Asn and Gln, and oxidation on Met.

Differences in the mass spectra for peptides found in the unmodified HSA and HSAMA samples were used to identify regions modified by methacryloylation reactions. However, since the search space is small, the search could also yield potential false positive sites in unmodified HSA. Such sites were used to control for and remove false positive modifications from the HSAMA samples. High sequence coverage of 92.45% and 91.95% was obtained for unmodified HSA upon tryptic and GluC digestion, respectively (Table 1), confirming digestion efficiency.

Modified Lys residues can hamper trypsin digestion[52]. In certain studies, Lys derivatization has indeed been used as a trypsin-blocking strategy to facilitate mass spectrometric analysis of certain Lys-rich proteins such as histones[53]. M9 and M10 samples were identified with higher sequence coverage when the methacryloylation search parameter was applied, confirming the presence of this chemical alteration of Lys residues at various sites. When

methacryloylation on Lys only was included in the database search, the sequence coverage by trypsin increased from 50% to 84% for M9 and from 42% to 89% for M10 batches. These results indicate that HSAMAs are heavily modified on lysine residues, and that some reduction in sequence coverage is due to the modification of other amino acid residues. The results of GluC search showed the same trend (Table 2). Expectedly, GluC digestion yielded a higher sequence coverage for modified batches compared to trypsin, as modified Lys could not be efficiently cleaved with trypsin.

The unique advantage of LC-MS/MS analysis is the capability to directly recognize chemically modified amino acid residues in fragment ion spectra. “VSKLVTDLTKVHTE” peptide spectra with and without methacryloylation on Lys are shown as a representative modification (Figure S1 of the SI).

We confined our results to modifications identified with ≥99% confidence. Table 2 summarizes high-confidence modifications noted in HSAMA batches with both tryptic and GluC digests, after removing false positives. Expectedly, GluC digestion generally resulted in identification of more modifications.

The analysis shows a total of 102 unambiguous modification sites on both M9 and M10 batches, although some modification sites differed between the two batches. Note that this is due to the presence of different modified peptide pools and does not necessarily imply that every HSA molecule is carrying all these modifications. This is also in line with the polydispersity observed in our MALDI-TOF-MS analysis (Figure S1). Since the majority (around 61% total) of modified sites are Lys, our findings also support the contention that Lys has a higher reactivity with MAA than other amino acids.

The modification sites identified under trypsin and GluC were complementary. While 24 modification sites for M9 and 26 sites for M10 were overlapping under both trypsin and GluC digestion, the majority of sites were uniquely identified in either trypsin or GluC digestion, showing their complementarity. In total, 19 sites were identified in all the analyses for M9 and M10. In M9 and M10 batches, 53 shared sites were identified using trypsin. GluC digestion similarly identified 55 shared modification sites in M9 and M10 batches.

To evaluate Lys residues with regards to solvent accessibility, we used the crystal structure of HSA at 2.5Å resolution (1AO6) on the Protein Data Bank (DOI:10.2210/pdb1AO6/pdb) to render its Gaussian surface representation in the 3D View function and highlighted the accessibility of Lys residues as provided by the Accessible Surface Area function (Figure 1 and Movie S1 of the SI).

We visualized the modification sites along the HSA sequence, also depicting solvent accessibility for Lys (Figure 2 a,b for M10 and M9). The length of the branches in Figure 2 a,b is a measure of Lys solvent accessibility on a relative scale (length 1 least to length 5 most accessible Lys). Some of the Lys residues known to be in the HSA interior were also modified, supporting our previous claim. Finally Figure 2 c and d show all the high-confidence methacryloylation sites on Lys, Cys, Thr, Ser, and Tyr along the M10 and M9 batches, as assessed by GluC and trypsin digestion separately.

The methacryloylation process for proteins involves multiple steps of mechanical mixing, pH changes, dialysis, freeze-drying, and interaction with the surface of the reaction flask or container. These process steps may induce alterations in physical characteristics such as increased molecular weight and aggregation, reduction in bioactivity, or even cause immunogenicity[54]. This chemistry is most often used for the preparation of gelatin methacryloyl, a known hydrogel for many biomedical applications[55]. Nevertheless, gelatin is already made of a heterogenous mixture of collagen fragments obtained via hydrolytic or enzymatic degradation of fibrous collagen[56]. Hence its physical characteristics or aggregation state may be less critical compared to a functional transporter protein such as HSA. To further assess the purity of HSA and HSAMA, structure and aggregation state in buffer, we used fast protein liquid chromatography (FPLC), a form of size exclusion chromatography often used to analyze or purify mixtures of proteins. The chromatogram of HSA and HSAMA is shown in Figure 3, which was in agreement with the MALDI-TOF-MS results. In the solution state, HSA was mainly in monomeric form; however, it also contained a small number of higher oligomers.

Although native HSA can naturally contain some dimers or oligomers, post-processing can also contribute to oligomerization[57]. For example, since commercial HSA is often prepared by a cold alcohol fractional process from pooled human plasma[58], this may also contribute to the generation of small amounts of dimers or higher oligomers in HSA or often oxidation of its free cysteine residue at position 34. In the present study, the HSAMA mainly formed dimers and a small amount of higher oligomers in buffer solution. Dimerization or oligomerization is a function of concentration and is largely dependent on hydrophobic and hydrogen bonding interactions[54, 59]. HSA dimers are either formed via covalent linking of Cys-34 or *via* non-covalent linking when subjected to extreme conditions[57].

We applied a high molar ratio of MAA to the HSA lysines to ensure that the maximum possible number of lysine residues are modified with methacryloyl groups. Lysine residues are positively charged in HSA, and modification with linear or cyclic anhydride such as succinic or acetic anhydride has been shown to alter the free energy and spatial confirmation of HSA, yielding a more negatively charged HSA and a reduced α-helical content[60]. Nevertheless, the degree and extent of α-helical loss content are dependent on the type of acylation reagent and reaction conditions. For example, Tayyab *et al.* showed that 87% acetylated HSA lost 33% of its α-helical content, while in a similar reaction, BSA-MA was shown to remain largely unaffected, with a minimal decrease (6%) in its α-helical content[35]. Hence it is possible that the individual structure of monomers in dimers is retained. However, further studies are needed to determine whether the dimers are formed via the crosslinking of Cys-34 on HSAMA or simply through physical forces such as hydrophobic-hydrophobic interactions.

The HSA hydrogel was prepared at three concentrations (11, 15, and 18% w/w) by photopolymerization of methacrylate HSA using UV light at an intensity of 6 mW/cm^2 for a duration of 10 min using a water-soluble LAP photoinitiator. The resulting hydrogels were then characterized using a swelling study. The degree of swelling and water content are critical factors influencing a hydrogel's mechanical properties, degradation, and release of leachables or cargo. Figures 4 A and C show the degree of hydrogel swelling and the

corresponding gel fraction. A low concentration of HSAMA (11% w/w) yielded a soft, putty-like hydrogel, and since handling was not possible, the swelling ratio and gel fraction were not measured. Albumin hydrogels reached their equilibrium swelling ratio, which was dependent on the initial concentration of the macromer. The degree of swelling of the hydrogels is regulated by their crosslinked density, which depends on the concentration of cross-linkable groups[61]. Hence the crosslinked density can be tuned by either varying the degree of methacrylate modification in the protein or altering the concentration of polymerizable groups.

We manipulated the concentration of HSAMA to control the crosslinked density, water uptake, and microstructure of the resulting hydrogels. Compared to two previous recent reports on photocrosslinked BSA hydrogels, the water uptake of our hydrogel at low concentration (15% w/w) was circa two times higher[33, 35]. However, increasing the HSAMA concentration to 18% w/w yielded a much denser network with a 2.4-fold reduced swelling ratio. The physicochemical properties of hydrogels are dependent on polymerization conditions such as the photoinitiator system, light intensity, irradiation time, amongst other variables. For example, in this study, we used LAP as a photoinitiator, whereas Irgacure 2959 has been used by other groups[33, 35]. Although LAP is usually preferred over Irgacure 2959 due to its water solubility and faster polymerization rate, a recent study using gelatin methacryloyl, LAP, and Irgacure 2959 showed that the swelling ratio of hydrogels is not affected by the type of the initiator[62]. However, the hydrogel in this research was prepared using much lower UV light intensity, circa 6 $mW.cm^{-2}$ compared to 150 and 700 $mW.cm^{-2}$.

Here the concentration of initiator was 1% (w/w), two times higher than previous studies. The polymerization propagation rate is proportional to the concentration of monomer radicals and initiator radicals. Hence, light intensity and initiator concentration are key parameters affecting kinetic chain length, which is inversely proportional to the initiation rate and, therefore, to the rate of polymerization[63]. Accordingly, due to different network architecture and crosslink density, the hydrogel demonstrated distinct physical properties, including swelling ratio.

Not all functional groups are involved in the polymerization reaction, and unrelated fractions or short chains not connected to the network will alter the physicochemical properties of the hydrogel or even produce undesired biological responses. Figure 3 shows the sol fraction of the hydrogels, confirming that increasing the HSAMA concentration from 15 to 18% w/w produced a denser network, as the sol fraction was reduced from 5.85 to 2.19%. Due to the importance of the sol fraction, especially to the biological and biocompatibility response, we analyzed its composition by SEC. The sol fraction (from 15% w/w sample) consisted of non-reacted HSAMA macromer and low-molecular-weight fragments with a peak molecular weight of 356 Da (Figure 4D). Long-wave UV (UVA) at low intensities and exposure time may not have sufficient energy to induce chain secession in the protein. For example, after 1h exposure of silk protein at an intensity of 2.37 ± 2.12 $mWcm^{-2}$ to UV light at 365 nm, no newly formed N-terminal amine groups could be detected by TNBS assay[64]. Nevertheless, in the presence of a photoinitiator, the generated radicals can induce photodegradation or change the physicochemical properties of proteins. For instance, BSA has been known to release free amino acids when exposed to oxidizing agents such as hydroxyl radicals, which

can be formed when water is present in the photopolymerization medium[65]. Although we did not analyze the composition of this sol fraction, it is probably composed of albumin oxidation products and amino acids, as suggested by the molecular weights of residues determined by SEC.

The samples turned to pale yellow after UV irradiation (Figure 5). Though LAP is known to exhibit low yellowing,[66] the yellow discoloration is probably due to the formation of chromophores such as hydroperoxide[67]. We noticed that photo yellowing was reversible, and a few hours after UV exposure or soaking in water, the samples were colorless.

The porosity of a hydrogel is a crucial factor that not only influences its mechanical properties but also regulates the diffusion of nutrients, waste removal from encapsulated cells, and its biodegradation rate as well as tissue ingrowth and vascularization[68]. Depending on the type and architecture of monomer or macromer, hydrogel porosity can be tuned by changing the molecular weight of the macromer or degree of side chain functionalization[69]. For example, reducing molar mass in the case of telechelic oligomer end-functionalized with acrylate or methacrylate groups results in lower hydrogel porosity[70]. As another example, in the case of side-chain-functionalized precursors, hydrogel porosity is controlled mainly by the degree of functionalization as shown for BSA or other hydrogels[33, 71]. Alternatively, hydrogel porosity can also be controlled by macromer concentration. We used three different concentrations to explore the effect of HSAMA concentration on hydrogel porosity. The hydrogels were dried with a critical point dryer to maintain the pore structure intact, and the pore structures as observed by SEM were uniform and fairly distributed along with the matrix. Hydrogels with low concentrations of 11% (w/w) had a thin wall and showed numerous small pores with an average size of 10.13± 3.79 μm. However, increasing the concentration of HSAMA to 15 and 18 % (w/w) thickened the cell walls, and the hydrogel average pore size was also increased to 20.04±5.45 and 44.9± 21.6 μm, respectively. As SEM images also confirmed, the resulting hydrogel was less porous compared to hydrogels with lower concentrations of HSAMA. Scaffold architecture and pore size can directly affect cell behavior and especially cellular proliferation and differentiation, as they provide mechanical and biological cues that regulate cell-matrix interactions[72]. The optimum value for scaffold pore size is cell-specific and also depends on the physicochemical priorities of the material[73]. For example, crosslinked collagen-glycosaminoglycan scaffold with pore size 20–125 μm has been reported to support partial morphogenesis of skin in a Guinea pig model[74]. Therefore, HSAMA concentration can be an effective tool to adjust the physicochemical properties of hydrogel, especially pore size and distribution, to meet the requirements of cell proliferation and infiltration.

When designing hydrogel scaffolds for tissue engineering, hydrogel degradation rate plays a crucial role, since there should be a match between scaffold replacement and tissue regeneration. In addition, hydrogels and their degradation products should elicit minimal foreign body response. Degradation of albumin hydrogels is dependent on the preparation method, and the degree of protein modification can determine its degradation rate and biocompatibility[22]. Natural and endogenous HSA has a half-life of 19 days and can degrade in any tissue through proteolytic enzymes. However, its degradation mainly takes place in the liver and kidney[14]. Synthetic albumin hydrogels, on the other hand, can display a

wide variety of physicochemical characteristics, as well as a wide range of degradation profiles ranging from fast-dissolving gels to long-lasting hydrogels. In fact, the physical parameters of gels such as microstructure, porosity, and elastic modulus can influence the behavior of macrophages and other phagocytic cells and hence alter the degradation rate of synthetic albumin-based gels. For example, while BSA gels prepared by pH-induced BSA significantly degraded after 4 weeks of subcutaneous implantation in Sprague–Dawley rats, their thermally denatured BSA counterparts showed no signs of degradation[17].

Alternatively, alterations in albumin structure or its modifications may also trigger its biodegradation or recycling via receptor-mediated endocytosis followed by lysosomal degradation through Gp18 and Gp30 receptor expressed on endothelial cell membranes of liver cells or peritoneal macrophages[75]. In fact, it has been shown that albumin modified by common crosslinker molecules such as formaldehyde or maleic anhydride have much higher affinity for Gp18 and Gp30 compared to native albumin[76].

Here we used bovine trypsin and *in vitro* enzymatic degradation of both 100% methacrylated HSA macromer; the resulting hydrogels were evaluated by SEC, spectroscopy, and gravimetry. Trypsin is one of the main digestive enzymes that catalyze proteolysis in vertebrates. Trypsin has a well-established role in proteomics studies, biochemical investigations, as well as *in vitro* degradation studies of protein-based biomaterials[77–78]. In our initial study, we used porcine-derived trypsin-EDTA used in cell culture (Gibco). However, our preliminary SEC studies showed that this trypsin was a mixture of components, probably a cocktail of proleptic enzymes. Hence, to facilitate the identification of the degradation products, we used pure bovine trypsin, which was TPCK-treated to inhibit the chymotrypsin.

To eliminate the interference of the sol fraction in the degradation study, the gels were first extracted in water to ensure that any weight reduction was the result of degradation. As expected, hydrogel mass was reduced 55% after 5 days of incubation in trypsin solution. The protein concentration of the supernatant was also measured by UV spectroscopy (Nanodrop). We observed a 1.9-fold increase in protein concentration, which provided further evidence for ongoing proteolytic and degradation activity. However, the degradation rate decreased over the study course, and after five days' incubation with the hydrogel, mass was reduced by only 3%, culminating in a total weight reduction of 58% after 10-day incubation in tryptic solution. Similarly, the protein concentration of the solution was only slightly increased (17%) after five additional days of incubation.

Previous studies of radically crosslinked BSA gels have shown that the degree of methacryloylation and concentration has a significant effect on the enzymatic degradation rate of BSA hydrogels[33, 35]. Consistent with these studies, our results showed that hydrogels synthesized with 100% methacrylated HSA may have increased resistance to enzymatic degradation, probably due to higher crosslink density or reduced reactivity toward proteolytic enzyme.

To further explore the effect of methacryloylation on enzymatic degradation of the HSA, we analyzed the degradation supernatant of HSAMA and the hydrogel by SEC (Figure 6

C and D). The chromatogram of trypsin-treated HSA showed five short fragments with a molar mass of 3363, 1438, and 665 Da and two monomeric components with molar mass of 258 and 105 Da. Some intact HSA was also detected in the chromatogram. Trypsin-treated HSAMA showed a degradation pattern relatively similar to that of HSA, and fragments with a molar mass of 3363, 1438, and 665 Da were common to both HSA and methacrylated HSA. However, the degradation fragments were also composed of very large aggregates, and monomeric fragments with a molar mass of 258 Da were absent from the spectra of HSAMA. These results support the notion that methacryloylation of albumin affects its susceptibility to tryptic digestion. The trypsin binding pocket is suitable for the ionic bonding of long side chain and positively charged residues such as lysine and arginine. Hence, trypsin exclusively cleaves the C-terminal of these residues[79]. Methacryloylation mainly targets lysine residues and removes the positive charge from the N-terminal amino group. Moreover, methacryloylation also alters the hydrophobic characteristic of HSA[80]. Therefore, it is possible that trypsin cleavage is reduced or even blocked. This finding is corroborated by the results of other studies on BSA, indicating that reduced degradation of fully methacrylated albumin gel may be partially related to altered enzyme activity on the hydrogel. When comparing these studies, it should also be noted that degradation kinetics is also dependent on enzyme sources. For example, despite the fact the trypsin from bovine and porcine share high similar sequence identity, their activity is different[81].

SEC analysis of degradation products from hydrogels (Figure 6D) demonstrated that the fragmentation pattern was similar to that of HSA, and the chromatogram showed four oligomeric and monomeric peptide fragments with a molar mass of 2154, 1400, 657, and 100 Da. The degradation product from day 1 was also similar to day 2, indicating continuous proteolytic action of trypsin. The supernatant from water degradation medium had no detectable protein, showing the stability of the albumin hydrogel in an aqueous medium within the period of our study. This was in good agreement with our protein concentration study (Figure 6B).

Albumin is a biocompatible and bioactive protein and is the major constituent of fetal bovine serum (FBS), which is ubiquitously used as an *in vitro* cell culture medium[82]. Despite this long history of biocompatibility, modification of albumin with methacrylate groups may change its biocompatibility profile, considering the fact that most methacrylate groups are generally considered to induce cytotoxicity[83]. It should be noted that the toxicity of methacrylated groups reduces after polymerization, and the resulting polymer with polymethacrylate chain is considered biocompatible. Nevertheless, since the polymerization is barely complete, the unreacted macromer may leach out and induce toxicity during cell-culture studies. Moreover, during cell encapsulation and 3D printing, cells are in brief contact with the macromers, which may reduce cell viability.

In this study, we investigated the cytocompatibility of the HSAMA macromers using the HMC3 human microglial cell line, immortalized using the SV40 virus. Because this cell line responds well to different pro-inflammatory stimuli, we used it to investigate the toxicity as well as the inflammatory response of both the HSAMA macromer and the resulting hydrogel[84].

The addition of albumin to the cell culture medium can have a regulatory effect on cell function. For example it has been shown that albumin at a concentration of (1.0 mg/mL) can significantly increase the osteoblastic activity in mouse osteoblastic cell lines (MC3T3-E1)[85]. Toxicity and mitochondrial activity were assessed after adding the HSAMA macromer and HSA at various concentrations ranging from 10 mg/ml to 0.625 mg/mL (Figure 7 A–B). Overall, there was no significant difference between the cell viability of HSA and corresponding HSAMA at the studied concentrations. For comparison, we also investigated the toxicity of gelatin methacryloyl (gelMA) macromer, a well-established macromer for cell encapsulation and hydrogel preparation. Interestingly, there was no significant difference in cell viability among control, gelMA, and HSA and its methacrylated derivative.

We note that preconditioned cell culture medium containing the leachable from photocrosslinking hydrogels seemed to have some degree of toxicity at high concentration and with no dilution. As discussed above, the composition of leachable was mainly unreacted HSAMA, some shorter peptide fragments, and possibly some residual photoinitiator Therefore, it is possible that the observed reduction in cell viability is a synergistic and concentration-dependent combination of the toxicity of the constituent residuals, such as the LAP photo initiator. For example, it was shown that pristine LAP at a concentration >10 mmol/L is toxic to mouse M-1 collecting duct cell monolayers[86]. In this study, we used a high concentration of the LAP photoinitiator (1% w/w) and a long exposure time (10 min) to ensure maximum conversion and reduction of the sol fraction. Therefore, unreacted LAP and possible lithium ions associated with LAP may have induced some toxicity or reduced LAP activity, contributing to the observed cytotoxicity response[87].

The toxicity mechanism of methacrylate functionality may be related to its potential for adduct formation with glutathione (GSH), an important antioxidant in the cell which results in disrupting the cell capability in preventing damages induced by reactive oxygen species (ROS) such as free radicals[83]. As a result of oxidative stress, additional effects such as DNA damage and cell cycle disruption may occur, eventually leading to cell death.[88] Nevertheless, generalizations regarding the toxicity of the methacrylate are challenging, as different chemical structures will affect the extent and nature of glutathione-methacrylate adduct formation. In addition, other mechanisms such as direct binding to DNA may also contribute to toxicity[89]. For example, Ansteinsson *et al.* showed that common monomers used as dental materials such as hydroxyethyl methacrylate (HEMA), triethylenglycol-dimethacrylate (TEGDMA), bisphenol-A-glycidyl-dimethacrylate (BisGMA), glycerol-dimethacrylate (GDMA), and methyl-methacrylate (MMA) all are capable of forming an adduct with glutathione. However, the link between depletion of cell glutathione source and toxicity could not be established, suggesting that other mechanisms may be involved in the observed toxicity[83]. Although exploring the cytotoxicity mechanism(s) of HASMA is beyond the scope of this study, the lower toxicity of HSAMA compared to free methacrylate may be partly related to the innate capability of albumin to reduce toxicity. Albumin binds to toxic compounds, reduces their toxicity, and acts as a waste carrier. For example, the binding of albumin to bilirubin, the toxic product of heme breakdown, renders it nontoxic until it is delivered to the liver and eliminated through hepatic excretion[7]. Chemically crosslinked albumin hydrogels made

from BSA have also been shown to reduce the toxicity of ruthenium against liver cells[90]. Alternatively, methacrylated albumin may have limited ability for adduct formation with GSH or interaction with DNA, or free radical formation may be counteracted by the specific antioxidant capacities of HSA[91]. It has been shown that HMC3 cells can produce a considerable amount of ROS, and hence they may have greater innate resistance to free radicals generated by external oxidizers[84]. Further studies are needed to explore the details and mechanisms of HSAMA toxicity.

To further characterize the response of HMC3 cells to HSA and HSAMA, we analyzed their morphology by confocal microscopy 24 h after treatment with the materials. The cell nucleus and cytoskeleton were visualized by DAPI and Phalloidin staining, respectively. Confocal microscopy was performed on the HMC3 cells treated with different materials (Figure 7). Interestingly, HSAMA was well tolerated by these cells, and there was no significant difference in terms of morphology among control and HSA/HSAMA-treated cells. HMC3 cells were mostly globular and elongated, and compared to either HSA or HSAMA, there was no difference in the actin cytoskeleton structure. Generally, healthy HMC3 cells have been reported to show a combination of globular, bipolar, and elongated morphology[84]. These morphological studies also confirmed the nontoxic nature of modified HSA at the studied concentrations.

Cellular attachment to the surface of the biomaterials is crucial for cell migration, viability, and proliferation. Cells that appropriately adhere to the substrate will provide a healthy environment that promotes tissue integration. Attachments and the spreading of immune cells such as the macrophage to the biomaterial's surface is a critical factor in the inflammatory and wound healing responses, ultimately determining the fate of the biomaterial. For example, macrophages can produce a range of chemicals ranging from ROS damaging or eroding the surface to secreting chemotactic cytokines such as interleukin 1, contributing to chronic inflammation, fibrous capsulation, and foreign body reaction[92–94].

Confocal microscopy evaluated the attachment of HMC3 cells to the surface of the HSAMA gels and control glass slide at days 1, 3, and 5 of culture (Figure 8). HMC3 cells on the hydrogels were mostly globular with a few elongated cells with a migratory phenotype. The cells on the tissue culture–treated glass slide were more elongated with a visible F-actin filament network at day 1 of culture. Generally, healthy HMC3 cells have been reported to show a combination of globular, bipolar, and elongated morphology[84]. The glass slide groups showed typical HMC3 morphologies, while the cells in hydrogel groups covered only a few spots on the surface of the gels. These cells were mainly clumped together and did not spread, unlike the glass slide group 3- and 5-days post-seeding.

To quantitate cell adhesion to albumin hydrogels, cell perimeters, and cells, Feret diameters were measured. Cell spreading was determined through evaluating cell spreading area as calculated from the area of Bodipy-Phalloidin-labeled actin filaments and nucleus stained with Nuc650, a fluorescent DNA nuclear stain. Average cell spreading area was measured after binarization and thresholding of actin filament fluorescence gray level using ImageJ software. On day 1 after seeding, HMC3 cells were mainly round with narrow Feret diameter distribution and an average Feret diameter of 50 μm (Figure 9 A–C). HMC3 cells

on hydrogels had a much smaller average perimeter (150 μm vs. 300 μm). Cells grown on the glass slide had larger Feret diameter distribution, indicating that the surface properties of the glass slides are favorable for HMC3 attachment. After 3 days' culture, quantification of the number of adherent microglia on the surface indicated the HMC3 cells on the surface of the hydrogel grew and the average cells' Feret diameter and perimeters increased to 105 and 400 μm respectively. However, compared to cells grown on glass, cells grown on hydrogel remained smaller, and ultimately, after 5 days post-seeding, achieved <40% confluence.

Biomaterial-cell attachment is mediated through contact with or anchoring to focal contacts, which are mainly heterodimeric transmembrane proteins that contain α and β subunits called integrins. Integrin mediates the cell attachments to the surface of biomaterials by linking the cell membrane to the discrete peptide regions of the ECM component such as collagen or fibronectin[95]. Unlike ECM molecules, which are designed for cell attachment and have an inherent mechanism for recognition and binding to specific anchoring proteins, HSA is not considered a cell-adhesive molecule. The major receptors involved in HSA attachments or internalization are related to albumin hemostasis.

As a carrier molecule, albumin is extensively internalized by cells through pinocytosis. However, albumin is protected from lysosomal degradation by the neonatal Fc receptor (FcRn), a ubiquitously expressed cellular receptor, through a strictly regulated pH-dependent binding mechanism[96]. Changes in albumin structure result in alteration of FcRn binding and rapid degradation of the albumin in lysosomes. Some tumor cells, especially endothelial-originated tumor cells, have receptors such as the gp60 receptor, a 60 kDa glycoprotein (albondin), which facilitates the transport of the albumin inside the tumor[97].

According to the cell adhesion results, it appears that albumin hydrogels can support cell adhesion and proliferation to some extent, despite the absence of structural adhesive molecules such as fibronectin or peptide fragments such as RGD in the network. However, cell attachment was significantly lower in the HSAMA hydrogel–coated glass slide compared to the control glass slide. Cell proliferation and spreading doubled every two days, and some HMC3 cells preserved their elongated morphology upon spreading on the top of albumin hydrogels. HMC3 macrophages developed filopodia after five days in culture, which indicate the macrophage's attachments to the surface and its probing the surrounding environment (Figure 9-D).

Cell attachment to the surface of albumin hydrogels can be regulated through two pathways: passive absorption of some serum proteins or through a receptor-mediated process. For example, cell surface scavenger receptors in endothelial cell membranes of hepatic and peritoneal macrophages, gp 30 and gp 18, specifically interact with damaged albumin as a scavenging mechanism for albumin catabolism[14].

Albumin, a non-adhesion protein, is widely involved in surface passivation applications; albumin gels, however, are generally not known to support cell adhesion[98]. For examples, cell attachment to surfaces with adhesive molecules is an indirect process that progresses through rapid adsorption of serum proteins on the substrate acting as a spacer between the cells and substrate[99–100]. However, the BSA coating has been shown to reduce the

attachment of the microglial cells, possibly through establishing a low protein binding surface[93]. Albumin may have different conformation or even some degree of denaturation depending on its production method and purity level, both of which affect its passivation efficiency. For example, in a recent study by Junren Ma *et al.,* it was shown that a fat-free BSA coating created by heat shock fractionation on the surface of silica nanoparticles prevented absorption of proteins from FBS up to 80%. The passivation efficacy of full-fat BSA produced through cold ethanol fractioning followed by heat shock fractionation was about 40%[40].

Adhesion of the cells to albumin may imply some degree of denaturation, which would promote absorption of adhesive protein from the serum onto the hydrogel surface, mediating cellular attachment[98]. In fact, it has been reported that the degree of alteration in albumin conformity and specially loss of α-helix is directly proportional to platelet adhesion on the surface of biomaterials[101]. This could be the prevalent mechanism of action responsible for the attachment of the cells to albumin hydrogels. For example, published reports on attachment of human hepatocellular carcinoma cells and cardiac cells on albumin hydrogels have hypothesized that attachment is mediated through the absorption of adhesive molecules on the hydrogels[35, 102].

In this experiment, HMC3 macrophages seeded onto HSAMA hydrogel-covered glass slides or plain glass slide controls developed filopodia, which are indicative of the macrophages' surface attachments and ability to interact with the surrounding environment. These findings are corroborated by other studies supporting the idea that low protein binding surfaces such as BSA coatings decrease the attachment of the brain resident macrophages called microglial cells[93]. Although albumin coatings can be effective, the physical nature of surface absorption and the instability of the coating in the presence of biological fluids can limit its practical applications. Crosslinked albumin, on the other hand, is stable and possesses tunable physical and chemical properties that can effectively prevent or reduce macrophage attachment.

The inflammatory and wound healing responses to biomaterials is determined by the extent of macrophage adhesion and their cytokine-secretory capabilities. To further characterize macrophage behavior on the surface of the hydrogel, we examined the composition of the cytokines and chemokines produced by the HMC3 macrophages using multiplex analysis. The concentration of the cytokines produced in the media were measured for hydrogel-coated and control glass slide groups (Figure 10).

The differential expression of cytokine between groups can be seen in Figure 10. The level of 10 major cytokines released by HMC3 into the media on the hydrogel was (in order of decreasing concentration) IL-6 >M-CSF> MCP-1> IL-12p40> FGF-2> IL-8> IL-27> IL-1β>RANTES> EGF. The level of 10 major cytokines released into the media by cells cultured on glass was IL-6> IL-8> VEGF-A> MCP-1> PDGF-AA> GROα> IL-27> RANTES> IL-22> FGF-2. Macrophages exposed to inflammatory stimuli such as exogenous compounds on biomaterial surfaces secrete pro-inflammatory cytokines such as TNF, IL-1, IL-6, IL-8, and IL-12, Il-18, IL-23 and Il-27[103]. In this study, the glass slide group elicited a significantly higher ($p < 0.05$) release of IL-6, IL-8, and TNF α. The amount

of other key cytokines involved in the inflammatory reaction was also high in the plain glass slide group. For example, high levels of the chemoattractant cytokine MCP-1 were detected in glass slides groups (132 pg/mL). MCP-1 is one of the key chemokines that regulate migration and infiltration of monocytes/macrophages[104]. Interestingly, MCP-1 was reduced to 20 pg/mL for hydrogel groups, suggesting that cells on hydrogels are less capable of recruiting immune cells such as other macrophages or leukocytes towards the hydrogel, which could result in less severe inflammatory response. The levels of VEGF and PDGF in the glass slide group were also much higher than in the albumin hydrogel-coated group (303 pg/mL vs 2.5 pg/mL). These two cytokines are associated with the vascularization process and blood vessel formation[105]. The high concentrations of these cytokines along with high amounts of IL8 and IL 6 indicate high vascular activity, possibly facilitating angiogenesis at the site of inflammation[105–106]. The macrophages on the surface of the hydrogel were generally smaller in size compared to the glass groups, and had a round rather than spread shape as confirmed by morphology analysis (Figure 8). Macrophages with spherical morphology and a less spread shape have a less developed cytoskeletal organization especially at day 1, and are believed to be less active in an inflammatory environment compared to more spread cells with visibly organized cytoskeletons. This lower macrophage activity may ultimately improve the interaction of the materials with cells, resulting in less perception by inflammatory cells and mild or minimum foreign body reaction[107].

Interestingly, the addition of unpolymerized albumin methacrylate macromers also reduced the activity of two potent neutrophil chemoattractants, IL8 and growth-related oncogene (GRO) alpha. These chemokines, especially GRO alpha, are involved in wound healing, inflammation, angiogenesis, and tumorigenesis. Long-term elevated expression of these chemokines can result in tissue damage and even elevated angiogenesis and tumorigenesis[108]. It also appears that the HSAMA macromer can influence the production of another chemokine, eotaxin, which is a potent chemoattractant for eosinophils. Eosinophils are an important type of immunomodulatory cell capable of producing and releasing a wide range of cytokines and chemokines such as IL-10 and TGF-β, which can suppress the inflammatory cascade[109]. The complex immunomodulatory function of HSAMA macromer is beyond the scope of this study.

Furthermore, the biocompatibility and modulatory effect on angiogenesis of HSAMA and HSAMA-containing hydrogels were investigated *in vivo* using a chicken embryo model. The highly vascularized extraembryonic membrane (CAM) and vascularized yolk sac were directly exposed to a solution of HSAMA or a disc of HSAMA polymerized hydrogel. The mortality of the treated embryos and the development of blood vessels were evaluated daily for four days. Indicators of angiogenesis such as increased blood vessel density, total blood vessel length, and mean lacunarity were evaluated and quantified for the areas exposed to HSAMA or HSAMA gel.

Angiogenesis, the development of new blood vessels from a pre-existing vascular plexus, is a regulated, complex biological process that depends on integrating cellular proliferation, differentiation, and migration[110]. Angiogenesis is required for normal growth and wound

healing, and any dysregulated or pathological angiogenesis could result in several diseases such as impaired wound healing and cancer.

Figure 11-A displays microscopic images of blood vessels after treatment with HSAMA solution or HSAMA hydrogel compared to control. Blood vessels exposed to HSAMA gel showed no evidence of toxicity (such as blood vessel bleeding) and demonstrated a slightly enhanced development of fine blood vessels in the exposed area (Figure 11-A). Furthermore, chicken embryos treated with HSAMA gel had survival rates similar to untreated embryos after four days of treatment (82.6% vs. 87.5%, respectively, Supplementary Figure 2). Quantification of the effect of angiogenesis modulation was performed using AngioTool software and revealed a significant increase in the mean percentage of the total blood vessel length when compared to the control (133.3% vs. 96.7%, respectively, $p<0.05$) (Figure 11 B–C).

Corroborated by *in vitro* toxicity test results, the HSAMA solution demonstrated no evidence of toxicity; however, signs of inhibited angiogenesis were observed (Figure 11-A). The survival rate of chicken embryos treated with HSAMA was similar to that of embryos treated with HSAMA hydrogel or PBS after four days of treatment (Supplementary Figure 2). Quantification of angiogenic parameters revealed a significant decrease in total blood vessel length of the exposed area compared to control (60.1% vs. 96.7%, respectively, $p<0.05$). There was also a significant increase in mean lacunarity compared to control (197.0% vs. 121.5%, respectively, $p <0.05$) (Figure 11 B–C).

These results suggest that the HSAMA gel was biocompatible with the chicken embryo and did not significantly reduce survival. Furthermore, the HSAMA gel exhibited a slight pro-angiogenic effect, with the development of fine blood vessels. Quantification of the effect of the modulation of angiogenesis revealed a significant increase in the total blood vessel length; however, the observed increase in vessel area and decrease in lacunarity were not statistically significant when compared to the control.

Quantitative analysis of the vascular networks upon exposure to biomaterials was performed using AngioTool software, which computes several morphological and vascular patterns of blood vessels, including the overall size of the vascular network, total vessel area, and average vessel length, vascular density, and lacunarity. Total vessel area and total vessel length are strongly correlated with enhanced development of blood vessels. In contrast, lacunarity describes the distribution of gaps around vessels within an image; greater lacunarity means stronger inhibition of angiogenesis[111]. The modified albumin displayed high biocompatibility; however, inhibition of angiogenesis was observed in terms of total vessel length and lacunarity. Such inhibition could be related to the methacrylate moiety. As described previously in this study, HSAMA was biocompatible with macrophages; however, signs of toxicity *in vivo* cannot be excluded.

A previous study demonstrated that methacrylic acid/sodium styrene sulfonate-based copolymers inhibited cell adhesion and proliferation of human umbilical vein endothelial cells[112]. Though several aspects of the toxicity of methyl methacrylate have been discussed in the literature[113], methacrylate is frequently used in drug delivery applications[114–116].

In our study, the concentration of methacrylate in HSAMA is low. We propose that the observed anti-angiogeneic effect of HSAMA is most likely correlated to a methacrylate moiety; however, chicken embryos exposed to HSAMA or control did not show a significant difference in rate of mortality.

Conclusion

In this report, albumin hydrogels were synthesized through methacryloylation of human serum albumin by methacrylic anhydride followed by UV polymerization. For the first time, we studied the methacryloylation chemistry of human serum albumin at the amino acid level. Our results showed that the accessible and not solvent available lysine residues and other nucleophilic amino acid groups such as Ser, Tyr, and Thr groups can be modified by this chemistry. The results further showed that the methacryloylation of HSA affects its aggregation status in water as well as its enzymatic degradation behavior, probably by altering the affinity between the enzyme and albumin substrate. Interestingly, the crosslinked hydrogel and pure HSA showed similar enzymatic degradation profiles. Nevertheless, HSA degradation was not fully complete, suggesting that the presence of the native unmodified lysine is necessary for the cleavage activity of trypsin. Albumin is largely known as a passivation agent, hindering protein absorption and consequently cell adhesion. Our findings showed that HSA hydrogels reduce the attachment of macrophages. Therefore, these hydrogels present a potential low bonding surface with certain advantages such as stability over pure albumin. Moreover, the cytokine and chemokine analysis also showed that the macrophages grown on albumin hydrogels have significantly less immunological activity, producing an order of magnitude fewer inflammatory cytokines compared to control cells grown on tissue culture glass slides. Overall, this novel group of photocrosslinkable albumin hydrogels demonstrate exciting potential in wound healing and other applications where a low inflammatory coating with tunable physicochemical properties and low protein binding properties is desired.

Supplementary Material

Refer to Web version on PubMed Central for supplementary material.

Acknowledgements

This work is supported by the U.S. National Institute of Diabetes and Digestive and Kidney Diseases (grant DK131417-01). Protein identification were carried out by the Proteomics Biomedicum core facility, Karolinska Institutet (https://ki.se/en/mbb/proteomics-biomedicum). We acknowledge the support of Dr. Tony Schilmiller from Mass Spectrometry and Metabolomics Core at Michigan State University for assisting us in acquiring and interpreting the MALDI MS data. We also thank the Assay Development and Drug Discovery Core at Michigan State University for assisting in the size exclusion experiment. A.A.S. was supported by the Swedish Research Council (grant 2020-00687) and the Swedish Society of Medicine (grant SLS-961262, 1086 Stiftelsen Albert Nilssons forskningsfond). N.N.M was supported by a Fulbright Visiting Scholar Fellowship.

References

1. Drury JL; Mooney DJ, Hydrogels for tissue engineering: scaffold design variables and applications. Biomaterials 2003, 24 (24), 4337–4351. [PubMed: 12922147]
2. El-Sherbiny IM; Yacoub MH, Hydrogel scaffolds for tissue engineering: Progress and challenges. Glob Cardiol Sci Pract 2013, 2013 (3), 316–342. [PubMed: 24689032]

3. Mantha S; Pillai S; Khayambashi P; Upadhyay A; Zhang Y; Tao O; Pham HM; Tran SD, Smart Hydrogels in Tissue Engineering and Regenerative Medicine. Materials (Basel) 2019, 12 (20), 3323.
4. Gyles DA; Castro LD; Silva JOC; Ribeiro-Costa RM, A review of the designs and prominent biomedical advances of natural and synthetic hydrogel formulations. European Polymer Journal 2017, 88, 373–392.
5. Madduma-Bandarage USK; Madihally SV, Synthetic hydrogels: Synthesis, novel trends, and applications. Journal of Applied Polymer Science 2021, 138 (19), 50376.
6. Catoira MC; Fusaro L; Di Francesco D; Ramella M; Boccafoschi F, Overview of natural hydrogels for regenerative medicine applications. Journal of Materials Science: Materials in Medicine 2019, 30 (10), 115. [PubMed: 31599365]
7. Merlot AM; Kalinowski DS; Richardson DR, Unraveling the mysteries of serum albumin—more than just a serum protein. Frontiers in Physiology 2014, 5 (299).
8. Aldecoa C; Llau JV; Nuvials X; Artigas A, Role of albumin in the preservation of endothelial glycocalyx integrity and the microcirculation: a review. Ann Intensive Care 2020, 10 (1), 85–85. [PubMed: 32572647]
9. Mazzaferro EM; Edwards T, Update on Albumin Therapy in Critical Illness. The Veterinary clinics of North America. Small animal practice 2020, 50 (6), 1289–1305. [PubMed: 32839002]
10. Mazzaferro EM; Edwards T, Update on Albumin Therapy in Critical Illness. Veterinary Clinics of North America: Small Animal Practice 2020, 50 (6), 1289–1305. [PubMed: 32839002]
11. Rozga J; Piatek T; Malkowski P, Human albumin: old, new, and emerging applications. Annals of transplantation 2013, 18, 205–17. [PubMed: 23792522]
12. Fanali G; di Masi A; Trezza V; Marino M; Fasano M; Ascenzi P, Human serum albumin: from bench to bedside. Molecular aspects of medicine 2012, 33 (3), 209–90. [PubMed: 22230555]
13. Rozga J; Piątek T; Małkowski P, Human albumin: old, new, and emerging applications. Annals of transplantation 2013, 18, 205–17. [PubMed: 23792522]
14. Spada A; Emami J; Tuszynski JA; Lavasanifar A, The Uniqueness of Albumin as a Carrier in Nanodrug Delivery. Molecular pharmaceutics 2021, 18 (5), 1862–1894. [PubMed: 33787270]
15. Bhamidipati CM; Coselli JS; LeMaire SA, BioGlue in 2011: what is its role in cardiac surgery? J Extra Corpor Technol 2012, 44 (1), P6–P12. [PubMed: 22730865]
16. Fuller C, Reduction of intraoperative air leaks with Progel in pulmonary resection: a comprehensive review. J Cardiothorac Surg 2013, 8, 90–90. [PubMed: 23590942]
17. Baler K; Michael R; Szleifer I; Ameer GA, Albumin hydrogels formed by electrostatically triggered self-assembly and their drug delivery capability. Biomacromolecules 2014, 15 (10), 3625–3633. [PubMed: 25148603]
18. Li P-S; Liang Lee I; Yu W-L; Sun J-S; Jane W-N; Shen H-H, A Novel Albumin-Based Tissue Scaffold for Autogenic Tissue Engineering Applications. Scientific Reports 2014, 4 (1), 5600. [PubMed: 25034369]
19. Hsu C-C; Serio A; Amdursky N; Besnard C; Stevens MM, Fabrication of Hemin-Doped Serum Albumin-Based Fibrous Scaffolds for Neural Tissue Engineering Applications. ACS Applied Materials & Interfaces 2018, 10 (6), 5305–5317. [PubMed: 29381329]
20. Biodegradable Scaffold Fabricated of Electrospun Albumin Fibers: Mechanical and Biological Characterization. Tissue Engineering Part C: Methods 2013, 19 (4), 257–264. [PubMed: 22881713]
21. Amdursky N; Mazo MM; Thomas MR; Humphrey EJ; Puetzer JL; St-Pierre J-P; Skaalure SC; Richardson RM; Terracciano CM; Stevens MM, Elastic serum-albumin based hydrogels: mechanism of formation and application in cardiac tissue engineering. Journal of Materials Chemistry B 2018, 6 (35), 5604–5612. [PubMed: 30283632]
22. Ong J; Zhao J; Justin AW; Markaki AE, Albumin-based hydrogels for regenerative engineering and cell transplantation. Biotechnol Bioeng 2019, 116 (12), 3457–3468. [PubMed: 31520415]
23. Gallego L; Junquera L; Meana A; García E; García V, Three-dimensional culture of mandibular human osteoblasts on a novel albumin scaffold: growth, proliferation, and differentiation potential in vitro. The International journal of oral & maxillofacial implants 2010, 25 (4), 699–705. [PubMed: 20657864]

24. Sun Y; Huang Y, Disulfide-crosslinked albumin hydrogels. Journal of Materials Chemistry B 2016, 4 (16), 2768–2775. [PubMed: 32263341]
25. Gao Y; Kieltyka RE; Jesse W; Norder B; Korobko AV; Kros A, Thiolated human serum albumin cross-linked dextran hydrogels as a macroscale delivery system. Soft Matter 2014, 10 (27), 4869–4874. [PubMed: 24866323]
26. Kim I; Choi JS; Lee S; Byeon HJ; Lee ES; Shin BS; Choi HG; Lee KC; Youn YS, In situ facile-forming PEG cross-linked albumin hydrogels loaded with an apoptotic TRAIL protein. Journal of controlled release : official journal of the Controlled Release Society 2015, 214, 30–9. [PubMed: 26188152]
27. Luo R; Lin M; Zhang C; Shi J; Zhang S; Chen Q; Hu Y; Zhang M; Zhang J; Gao F, Genipin-crosslinked human serum albumin coating using a tannic acid layer for enhanced oral administration of curcumin in the treatment of ulcerative colitis. Food Chemistry 2020, 330, 127241. [PubMed: 32540526]
28. Hayashi A; Takazawa H; Saika M, Heat-induced Gelation of Human Serum Albumin and Model Compounds. Agricultural and Biological Chemistry 1990, 54 (5), 1121–1127.
29. Arabi SH; Aghelnejad B; Schwieger C; Meister A; Kerth A; Hinderberger D, Serum albumin hydrogels in broad pH and temperature ranges: characterization of their self-assembled structures and nanoscopic and macroscopic properties. Biomaterials Science 2018, 6 (3), 478–492. [PubMed: 29446432]
30. Elzoghby AO; Samy WM; Elgindy NA, Albumin-based nanoparticles as potential controlled release drug delivery systems. Journal of Controlled Release 2012, 157 (2), 168–182. [PubMed: 21839127]
31. Bhattacharya M; Jain N; Bhasne K; Kumari V; Mukhopadhyay S, pH-Induced conformational isomerization of bovine serum albumin studied by extrinsic and intrinsic protein fluorescence. Journal of fluorescence 2011, 21 (3), 1083–90. [PubMed: 21128099]
32. Chen J; Dong Q; Huang Y; Ma X; Fan TH; Bian Z; O'Reilly Beringhs A; Lu X; Lei Y, Preparation, characterization and application of a protein hydrogel with rapid self-healing and unique autofluoresent multi-functionalities. Journal of biomedical materials research. Part A 2019, 107 (1), 81–91. [PubMed: 30408320]
33. Lantigua D; Nguyen MA; Wu X; Suvarnapathaki S; Kwon S; Gavin W; Camci-Unal G, Synthesis and characterization of photocrosslinkable albumin-based hydrogels for biomedical applications. Soft Matter 2020, 16 (40), 9242–9252. [PubMed: 32929420]
34. Iemma F; Spizzirri UG; Muzzalupo R; Puoci F; Trombino S; Picci N, Spherical hydrophilic microparticles obtained by the radical copolymerisation of functionalised bovine serum albumin. Colloid and Polymer Science 2004, 283 (3), 250–256.
35. Ferracci G; Zhu M; Ibrahim MS; Ma G; Fan TF; Lee BH; Cho N-J, Photocurable Albumin Methacryloyl Hydrogels as a Versatile Platform for Tissue Engineering. ACS Applied Bio Materials 2020, 3 (2), 920–934.
36. Smith PT; Narupai B; Tsui JH; Millik SC; Shafranek RT; Kim D-H; Nelson A, Additive Manufacturing of Bovine Serum Albumin-Based Hydrogels and Bioplastics. Biomacromolecules 2020, 21 (2), 484–492. [PubMed: 31714754]
37. Abbate V; Kong X; Bansal SS, Photocrosslinked bovine serum albumin hydrogels with partial retention of esterase activity. Enzyme and Microbial Technology 2012, 50 (2), 130–136. [PubMed: 22226199]
38. Peters T, Serum Albumin. In Advances in Protein Chemistry, Anfinsen CB; Edsall JT; Richards FM, Eds. Academic Press: 1985; Vol. 37, pp 161–245. [PubMed: 3904348]
39. Mulvihill JN; Faradji A; Oberling F; Cazenave JP, Surface passivation by human albumin of plasmapheresis circuits reduces platelet accumulation and thrombus formation. Experimental and clinical studies. Journal of biomedical materials research 1990, 24 (2), 155–63. [PubMed: 2329112]
40. Ma GJ; Ferhan AR; Jackman JA; Cho N-J, Conformational flexibility of fatty acid-free bovine serum albumin proteins enables superior antifouling coatings. Communications Materials 2020, 1 (1), 45.

41. Amiji M; Park K, Surface modification of polymeric biomaterials with poly(ethylene oxide), albumin, and heparin for reduced thrombogenicity. Journal of biomaterials science. Polymer edition 1993, 4 (3), 217–34. [PubMed: 8476792]
42. Tsui C; Koss K; Churchward MA; Todd KG, Biomaterials and glia: Progress on designs to modulate neuroinflammation. Acta Biomater 2019, 83, 13–28. [PubMed: 30414483]
43. Kain KH; Miller JWI; Jones-Paris CR; Thomason RT; Lewis JD; Bader DM; Barnett JV; Zijlstra A, The chick embryo as an expanding experimental model for cancer and cardiovascular research. Dev Dyn 2014, 243 (2), 216–228. [PubMed: 24357262]
44. Pawlikowska P; Tayoun T; Oulhen M; Faugeroux V; Rouffiac V; Aberlenc A; Pommier AL; Honore A; Marty V; Bawa O; Lacroix L; Scoazec JY; Chauchereau A; Laplace-Builhe C; Farace F, Exploitation of the chick embryo chorioallantoic membrane (CAM) as a platform for anti-metastatic drug testing. Scientific Reports 2020, 10 (1), 16876. [PubMed: 33037240]
45. Ribatti D, The chick embryo chorioallantoic membrane (CAM) assay. Reprod Toxicol 2017, 70, 97–101. [PubMed: 27832950]
46. Vlasova IM; Saletsky AM, Study of the denaturation of human serum albumin by sodium dodecyl sulfate using the intrinsic fluorescence of albumin. Journal of Applied Spectroscopy 2009, 76 (4), 536–541.
47. Iemma F; Spizzirri UG; Puoci F; Muzzalupo R; Trombino S; Picci N, Radical cross-linked albumin microspheres as potential drug delivery systems: preparation and in vitro studies. Drug delivery 2005, 12 (4), 229–34. [PubMed: 16036717]
48. Oakes J, Protein hydration. Nuclear magnetic resonance relaxation studies of the state of water in native bovine serum albumin solutions. Journal of the Chemical Society, Faraday Transactions 1: Physical Chemistry in Condensed Phases 1976, 72 (0), 216–227.
49. Wurm F; Steinbach T; Klok HA, One-pot squaric acid diester mediated aqueous protein conjugation. Chemical communications (Cambridge, England) 2013, 49 (71), 7815–7.
50. Koniev O; Wagner A, Developments and recent advancements in the field of endogenous amino acid selective bond forming reactions for bioconjugation. Chemical Society Reviews 2015, 44 (15), 5495–5551. [PubMed: 26000775]
51. Mir MM; Fazili KM; Abul Qasim M, Chemical modification of buried lysine residues of bovine serum albumin and its influence on protein conformation and bilirubin binding. Biochimica et biophysica acta 1992, 1119 (3), 261–7. [PubMed: 1547271]
52. Nie S; Lo A; Zhu J; Wu J; Ruffin MT; Lubman DM, Isobaric Protein-Level Labeling Strategy for Serum Glycoprotein Quantification Analysis by Liquid Chromatography–Tandem Mass Spectrometry. Analytical Chemistry 2013, 85 (11), 5353–5357. [PubMed: 23638883]
53. Garcia BA; Mollah S; Ueberheide BM; Busby SA; Muratore TL; Shabanowitz J; Hunt DF, Chemical derivatization of histones for facilitated analysis by mass spectrometry. Nature Protocols 2007, 2 (4), 933–938. [PubMed: 17446892]
54. Qian J; Tang Q; Cronin B; Markovich R; Rustum A, Development of a high performance size exclusion chromatography method to determine the stability of Human Serum Albumin in a lyophilized formulation of Interferon alfa-2b. Journal of Chromatography A 2008, 1194 (1), 48–56. [PubMed: 18258245]
55. Yue K; Li X; Schrobback K; Sheikhi A; Annabi N; Leijten J; Zhang W; Zhang YS; Hutmacher DW; Klein TJ; Khademhosseini A, Structural analysis of photocrosslinkable methacryloyl-modified protein derivatives. Biomaterials 2017, 139, 163–171. [PubMed: 28618346]
56. Liu XM; Herrick DZ; Maziarz EP In Analysis of gelatin using various separation and detection technologies, 2018.
57. Chubarov A; Spitsyna A; Krumkacheva O; Mitin D; Suvorov D; Tormyshev V; Fedin M; Bowman MK; Bagryanskaya E, Reversible Dimerization of Human Serum Albumin. Molecules (Basel, Switzerland) 2020, 26 (1).
58. Matejtschuk P; Dash CH; Gascoigne EW, Production of human albumin solution: a continually developing colloid. British journal of anaesthesia 2000, 85 (6), 887–95. [PubMed: 11732525]
59. Berkowitz SA, Role of analytical ultracentrifugation in assessing the aggregation of protein biopharmaceuticals. The AAPS Journal 2006, 8 (3), E590–E605. [PubMed: 17025277]

60. Tayyab S; Haq SK; Sabeeha; Aziz MA; Khan MM; Muzammil S, Effect of lysine modification on the conformation and indomethacin binding properties of human serum albumin. International journal of biological macromolecules 1999, 26 (2–3), 173–80. [PubMed: 10517526]
61. Lee S; Tong X; Yang F, The effects of varying poly(ethylene glycol) hydrogel crosslinking density and the crosslinking mechanism on protein accumulation in three-dimensional hydrogels. Acta Biomaterialia 2014, 10 (10), 4167–4174. [PubMed: 24887284]
62. Xu H; Casillas J; Krishnamoorthy S; Xu C, Effects of Irgacure 2959 and lithium phenyl-2,4,6-trimethylbenzoylphosphinate on cell viability, physical properties, and microstructure in 3D bioprinting of vascular-like constructs. Biomedical materials (Bristol, England) 2020, 15 (5), 055021.
63. Abedin F; Ye Q; Camarda K; Spencer P, Impact of light intensity on the polymerization kinetics and network structure of model hydrophobic and hydrophilic methacrylate based dental adhesive resin. Journal of Biomedical Materials Research Part B: Applied Biomaterials 2016, 104 (8), 1666–1678. [PubMed: 26340329]
64. Lee S; Kim SH; Jo Y-Y; Ju W-T; Kim H-B; Kweon H, Effects of Ultraviolet Light Irradiation on Silk Fibroin Films Prepared under Different Conditions. Biomolecules 2021, 11 (1), 70. [PubMed: 33430245]
65. Liu F; Lai S; Tong H; Lakey PSJ; Shiraiwa M; Weller MG; Pöschl U; Kampf CJ, Release of free amino acids upon oxidation of peptides and proteins by hydroxyl radicals. Analytical and Bioanalytical Chemistry 2017, 409 (9), 2411–2420. [PubMed: 28108753]
66. Linnenberger A; Bodine MI; Fiedler C; Roberts JJ; Skaalure SC; Quinn JP; Bryant SJ; Cole M; McLeod RR, Three dimensional live cell lithography. Opt. Express 2013, 21 (8), 10269–10277. [PubMed: 23609736]
67. Chiang TH; Hsieh T-E, Effect of tertiary amines on yellowing of UV-curable epoxide resins. Polymer International 2007, 56 (12), 1544–1552.
68. Annabi N; Nichol JW; Zhong X; Ji C; Koshy S; Khademhosseini A; Dehghani F, Controlling the porosity and microarchitecture of hydrogels for tissue engineering. Tissue Eng Part B Rev 2010, 16 (4), 371–383. [PubMed: 20121414]
69. Nicol E, Photopolymerized Porous Hydrogels. Biomacromolecules 2021, 22 (4), 1325–1345. [PubMed: 33793224]
70. Cruise GM; Scharp DS; Hubbell JA, Characterization of permeability and network structure of interfacially photopolymerized poly(ethylene glycol) diacrylate hydrogels. Biomaterials 1998, 19 (14), 1287–1294. [PubMed: 9720892]
71. Baier Leach J; Bivens KA; Patrick CW Jr.; Schmidt CE, Photocrosslinked hyaluronic acid hydrogels: natural, biodegradable tissue engineering scaffolds. Biotechnol Bioeng 2003, 82 (5), 578–89. [PubMed: 12652481]
72. Karande TS; Ong JL; Agrawal CM, Diffusion in Musculoskeletal Tissue Engineering Scaffolds: Design Issues Related to Porosity, Permeability, Architecture, and Nutrient Mixing. Annals of Biomedical Engineering 2004, 32 (12), 1728–1743. [PubMed: 15675684]
73. Loh QL; Choong C, Three-dimensional scaffolds for tissue engineering applications: role of porosity and pore size. Tissue Eng Part B Rev 2013, 19 (6), 485–502. [PubMed: 23672709]
74. Yannas IV; Lee E; Orgill DP; Skrabut EM; Murphy GF, Synthesis and characterization of a model extracellular matrix that induces partial regeneration of adult mammalian skin. Proc Natl Acad Sci U S A 1989, 86 (3), 933–937. [PubMed: 2915988]
75. Larsen MT; Kuhlmann M; Hvam ML; Howard KA, Albumin-based drug delivery: harnessing nature to cure disease. Mol Cell Ther 2016, 4, 3–3. [PubMed: 26925240]
76. Schnitzer JE; Bravo J, High affinity binding, endocytosis, and degradation of conformationally modified albumins. Potential role of gp30 and gp18 as novel scavenger receptors. The Journal of biological chemistry 1993, 268 (10), 7562–70. [PubMed: 8463286]
77. Vandermarliere E; Mueller M; Martens L, Getting intimate with trypsin, the leading protease in proteomics. Mass spectrometry reviews 2013, 32 (6), 453–65. [PubMed: 23775586]
78. Knipe JM; Chen F; Peppas NA, Enzymatic biodegradation of hydrogels for protein delivery targeted to the small intestine. Biomacromolecules 2015, 16 (3), 962–72. [PubMed: 25674922]

79. Olsen JV; Ong SE; Mann M, Trypsin cleaves exclusively C-terminal to arginine and lysine residues. Mol Cell Proteomics 2004, 3 (6), 608–14. [PubMed: 15034119]
80. Virág D; Dalmadi-Kiss B; Vékey K; Drahos L; Klebovich I; Antal I; Ludányi K, Current Trends in the Analysis of Post-translational Modifications. Chromatographia 2020, 83 (1), 1–10.
81. Walmsley SJ; Rudnick PA; Liang Y; Dong Q; Stein SE; Nesvizhskii AI, Comprehensive Analysis of Protein Digestion Using Six Trypsins Reveals the Origin of Trypsin As a Significant Source of Variability in Proteomics. Journal of Proteome Research 2013, 12 (12), 5666–5680. [PubMed: 24116745]
82. Zheng X; Baker H; Hancock WS; Fawaz F; McCaman M; Pungor E Jr., Proteomic Analysis for the Assessment of Different Lots of Fetal Bovine Serum as a Raw Material for Cell Culture. Part IV. Application of Proteomics to the Manufacture of Biological Drugs. Biotechnology Progress 2006, 22 (5), 1294–1300. [PubMed: 17022666]
83. Ansteinsson V; Kopperud HB; Morisbak E; Samuelsen JT, Cell toxicity of methacrylate monomers—The role of glutathione adduct formation. Journal of Biomedical Materials Research Part A 2013, 101 (12), 3504–3510. [PubMed: 23613115]
84. Dello Russo C; Cappoli N; Coletta I; Mezzogori D; Paciello F; Pozzoli G; Navarra P; Battaglia A, The human microglial HMC3 cell line: where do we stand? A systematic literature review. Journal of Neuroinflammation 2018, 15 (1), 259. [PubMed: 30200996]
85. Ishida K; Yamaguchi M, Role of albumin in osteoblastic cells: enhancement of cell proliferation and suppression of alkaline phosphatase activity. International journal of molecular medicine 2004, 14 (6), 1077–81. [PubMed: 15547677]
86. Nguyen AK; Goering PL; Elespuru RK; Sarkar Das S; Narayan RJ, The Photoinitiator Lithium Phenyl (2,4,6-Trimethylbenzoyl) Phosphinate with Exposure to 405 nm Light Is Cytotoxic to Mammalian Cells but Not Mutagenic in Bacterial Reverse Mutation Assays. Polymers 2020, 12 (7).
87. Young W, Review of Lithium Effects on Brain and Blood. Cell Transplantation 2009, 18 (9), 951–975. [PubMed: 19523343]
88. Schweikl H; Spagnuolo G; Schmalz G, Genetic and cellular toxicology of dental resin monomers. Journal of dental research 2006, 85 (10), 870–7. [PubMed: 16998124]
89. Wisniewska-Jarosinska M; Poplawski T; Chojnacki CJ; Pawlowska E; Krupa R; Szczepanska J; Blasiak J, Independent and combined cytotoxicity and genotoxicity of triethylene glycol dimethacrylate and urethane dimethacrylate. Mol Biol Rep 2011, 38 (7), 4603–11. [PubMed: 21127987]
90. Zhao Z; Hu R; Shi H; Wang Y; Ji L; Zhang P; Zhang Q, Design of ruthenium-albumin hydrogel for cancer therapeutics and luminescent imaging. Journal of Inorganic Biochemistry 2019, 194, 19–25. [PubMed: 30798078]
91. Taverna M; Marie A-L; Mira J-P; Guidet B, Specific antioxidant properties of human serum albumin. Ann Intensive Care 2013, 3 (1), 4–4. [PubMed: 23414610]
92. DeFife KM; Colton E; Nakayama Y; Matsuda T; Anderson JM, Spatial regulation and surface chemistry control of monocyte/macrophage adhesion and foreign body giant cell formation by photochemically micropatterned surfaces. Journal of biomedical materials research 1999, 45 (2), 148–54. [PubMed: 10397969]
93. Leung BK; Biran R; Underwood CJ; Tresco PA, Characterization of microglial attachment and cytokine release on biomaterials of differing surface chemistry. Biomaterials 2008, 29 (23), 3289–3297. [PubMed: 18485471]
94. Liu Y; Segura T, Biomaterials-Mediated Regulation of Macrophage Cell Fate. Front Bioeng Biotechnol 2020, 8, 609297–609297. [PubMed: 33363135]
95. Adam Hacking S; Khademhosseini A, Chapter II.1.3 - Cells and Surfaces in vitro. In Biomaterials Science (Third Edition), Ratner BD; Hoffman AS; Schoen FJ; Lemons JE, Eds. Academic Press: 2013; pp 408–427.
96. Sand KMK; Bern M; Nilsen J; Noordzij HT; Sandlie I; Andersen JT, Unraveling the Interaction between FcRn and Albumin: Opportunities for Design of Albumin-Based Therapeutics. Frontiers in Immunology 2015, 5 (682).

97. Vogel SM; Minshall RD; Pilipović M; Tiruppathi C; Malik AB, Albumin uptake and transcytosis in endothelial cells in vivo induced by albumin-binding protein. American Journal of Physiology-Lung Cellular and Molecular Physiology 2001, 281 (6), L1512–L1522. [PubMed: 11704548]

98. Hirose M; Tachibana A; Tanabe T, Recombinant human serum albumin hydrogel as a novel drug delivery vehicle. Materials Science and Engineering: C 2010, 30 (5), 664–669.

99. ANDRADE JD; HLADY V, Plasma Protein Adsorption: The Big Twelvea. Annals of the New York Academy of Sciences 1987, 516 (1), 158–172. [PubMed: 3439723]

100. Hacking SA; Khademhosseini A In Chapter II.1.3@ Cells and Surfaces in vitro, 2013.

101. Sivaraman B; Latour RA, The Adherence of platelets to adsorbed albumin by receptor-mediated recognition of binding sites exposed by adsorption-induced unfolding. Biomaterials 2010, 31 (6), 1036–1044. [PubMed: 19864017]

102. Fleischer S; Shapira A; Regev O; Nseir N; Zussman E; Dvir T, Albumin fiber scaffolds for engineering functional cardiac tissues. Biotechnology and Bioengineering 2014, 111 (6), 1246–1257. [PubMed: 24420414]

103. Arango Duque G; Descoteaux A, Macrophage Cytokines: Involvement in Immunity and Infectious Diseases. Frontiers in Immunology 2014, 5 (491).

104. Monocyte Chemoattractant Protein-1 (MCP-1): An Overview. Journal of Interferon & Cytokine Research 2009, 29 (6), 313–326. [PubMed: 19441883]

105. Angelo LS; Kurzrock R, Vascular Endothelial Growth Factor and Its Relationship to Inflammatory Mediators. Clinical Cancer Research 2007, 13 (10), 2825–2830. [PubMed: 17504979]

106. Wynn TA; Vannella KM, Macrophages in Tissue Repair, Regeneration, and Fibrosis. Immunity 2016, 44 (3), 450–462. [PubMed: 26982353]

107. Blakney AK; Swartzlander MD; Bryant SJ, The effects of substrate stiffness on the in vitro activation of macrophages and in vivo host response to poly(ethylene glycol)-based hydrogels. Journal of biomedical materials research. Part A 2012, 100 (6), 1375–1386. [PubMed: 22407522]

108. Fimmel S; Devermann L; Herrmann A; Zouboulis C, GRO-alpha: a potential marker for cancer and aging silenced by RNA interference. Ann N Y Acad Sci 2007, 1119, 176–89. [PubMed: 18056965]

109. Simon D; Simon H-U, Chapter 12 - Eosinophils. In Asthma and COPD (Second Edition), Barnes PJ; Drazen JM; Rennard SI; Thomson NC, Eds. Academic Press: Oxford, 2009; pp 145–156.

110. Adams RH; Alitalo K, Molecular regulation of angiogenesis and lymphangiogenesis. Nature Reviews Molecular Cell Biology 2007, 8 (6), 464–478. [PubMed: 17522591]

111. Gould DJ; Vadakkan TJ; Poché RA; Dickinson ME, Multifractal and lacunarity analysis of microvascular morphology and remodeling. Microcirculation 2011, 18 (2), 136–151. [PubMed: 21166933]

112. Guillou-Buffello DL; Chesneau C-I; Gindre M; HÈlary G; Laugier P; Migonney V, Inhibition of angiogenesis in vitro with soluble copolymers monitored with a quartz crystal resonator. Irbm 2010, 31, 271–279.

113. Gosavi SS; Gosavi SY; Alla RK, Local and systemic effects of unpolymerised monomers. Dent Res J (Isfahan) 2010, 7 (2), 82–87. [PubMed: 22013462]

114. Tarawneh O; Alwahsh W; Abul-Futouh H; Al-Samad LA; Hamadneh L; Abu Mahfouz H; Fadhil Abed A, Determination of Antimicrobial and Antibiofilm Activity of Combined LVX and AMP Impregnated in p(HEMA) Hydrogel. Applied Sciences 2021, 11 (18).

115. Bettencourt A; Almeida AJ, Poly(methyl methacrylate) particulate carriers in drug delivery. J Microencapsul 2012, 29 (4), 353–67. [PubMed: 22251239]

116. Cilurzo F; Selmin F; Gennari CG; Montanari L; Minghetti P, Application of methyl methacrylate copolymers to the development of transdermal or loco-regional drug delivery systems. Expert Opin Drug Deliv 2014, 11 (7), 1033–45. [PubMed: 24766369]

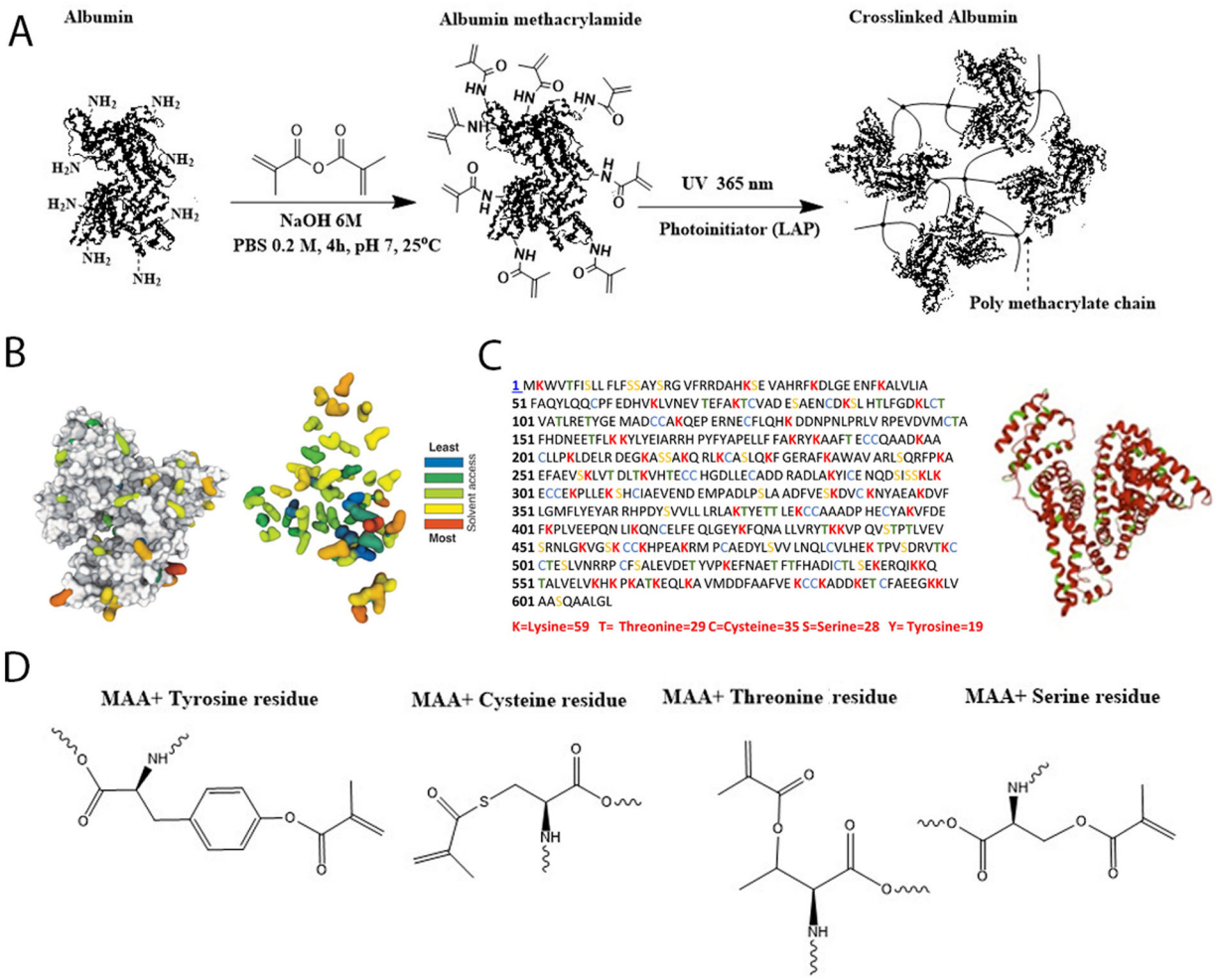

Figure 1.

A: Schematic depiction of the reaction of HSA with methacrylic anhydride. Middle-left: The amino acid sequences of HSA and the distribution of five amino acids, lysine (59), threonine (29), cysteine (35), serine (28), and tyrosine (19), in HSA. B: The crystal structure of HSA with lysine residues and the solvent accessibility of Lys residues in HSA sequence. About 20% of the lysine residues usually have no solution access. C: HSA structure was rendered based on PDB file 1AO6. D: The possible reaction of four amino acids in HSA (threonine, cysteine, serine, and tyrosine) with MAA is shown.

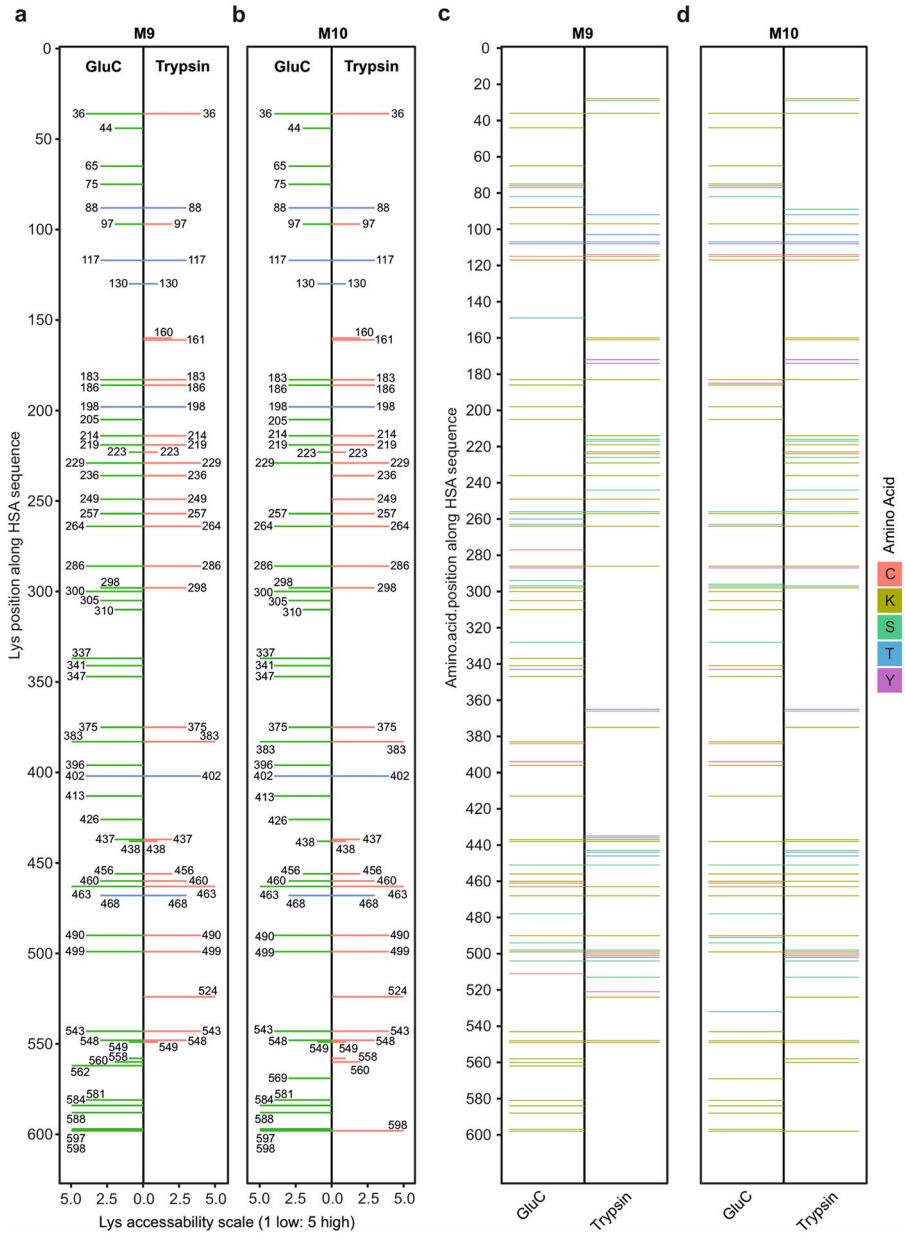

Figure 2.

Pine plots summarizing and visualizing the methacryloylation sites along the proteins' sequence identified with high confidence using GluC and trypsin digestion for M9 (a) and M10 (b). The green and pink branches represent sites identified with GluC and trypsin digestion, respectively. The number on the branches denotes the Lys residue position in the protein. The blue branches are those identified also on unmodified HSA and are thus considered false positive modifications. The Y axis shows the modified residues along the protein sequence, while the X axis represents the solvent accessibility of Lys on a scale of 1 (least accessible) to 5 (most accessible) based on crystal structure. **c** and **d)** the methacryloylation sites identified with high confidence on Lys, Cys, Thr, Ser and Tyr along

the proteins' sequence. The colors represent the amino acid residues, and the x axis scale is irrelevant in these two panels.

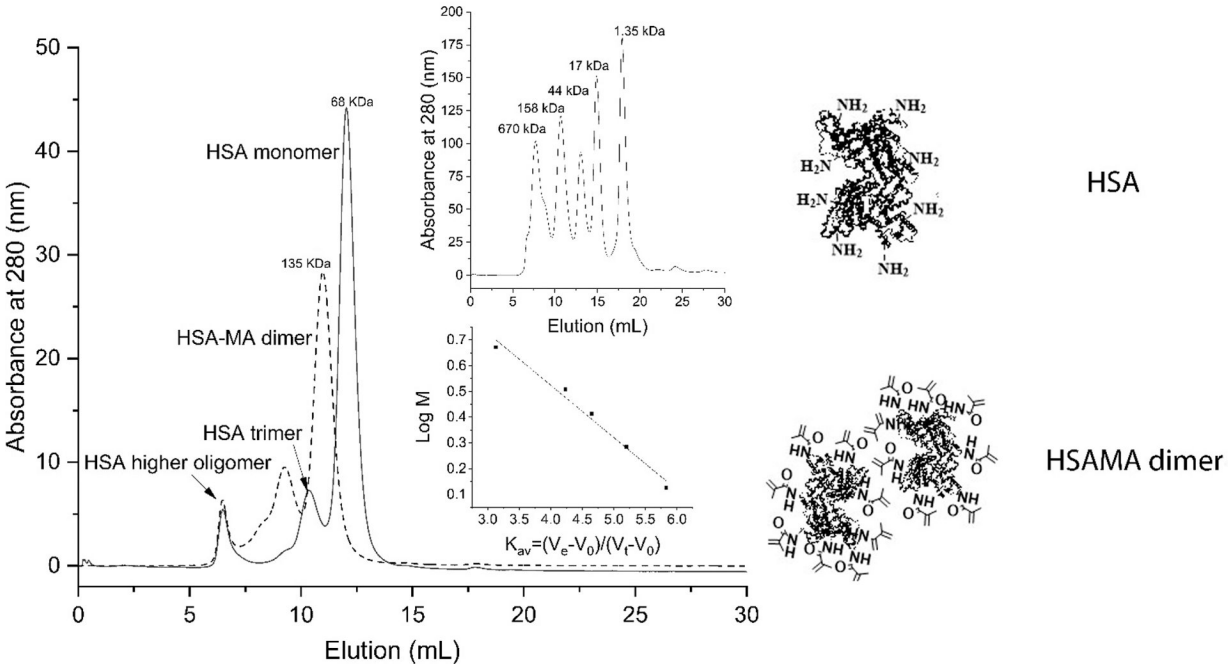

Figure 3.

SEC spectra of HSA and HSAMA. The picture insert shows the calibration standard and calibration curve used for calculating the molecular weight of HSA and HSAMA. The values of V_t and V_0 for the used column were 24 and 5.5, respectively.

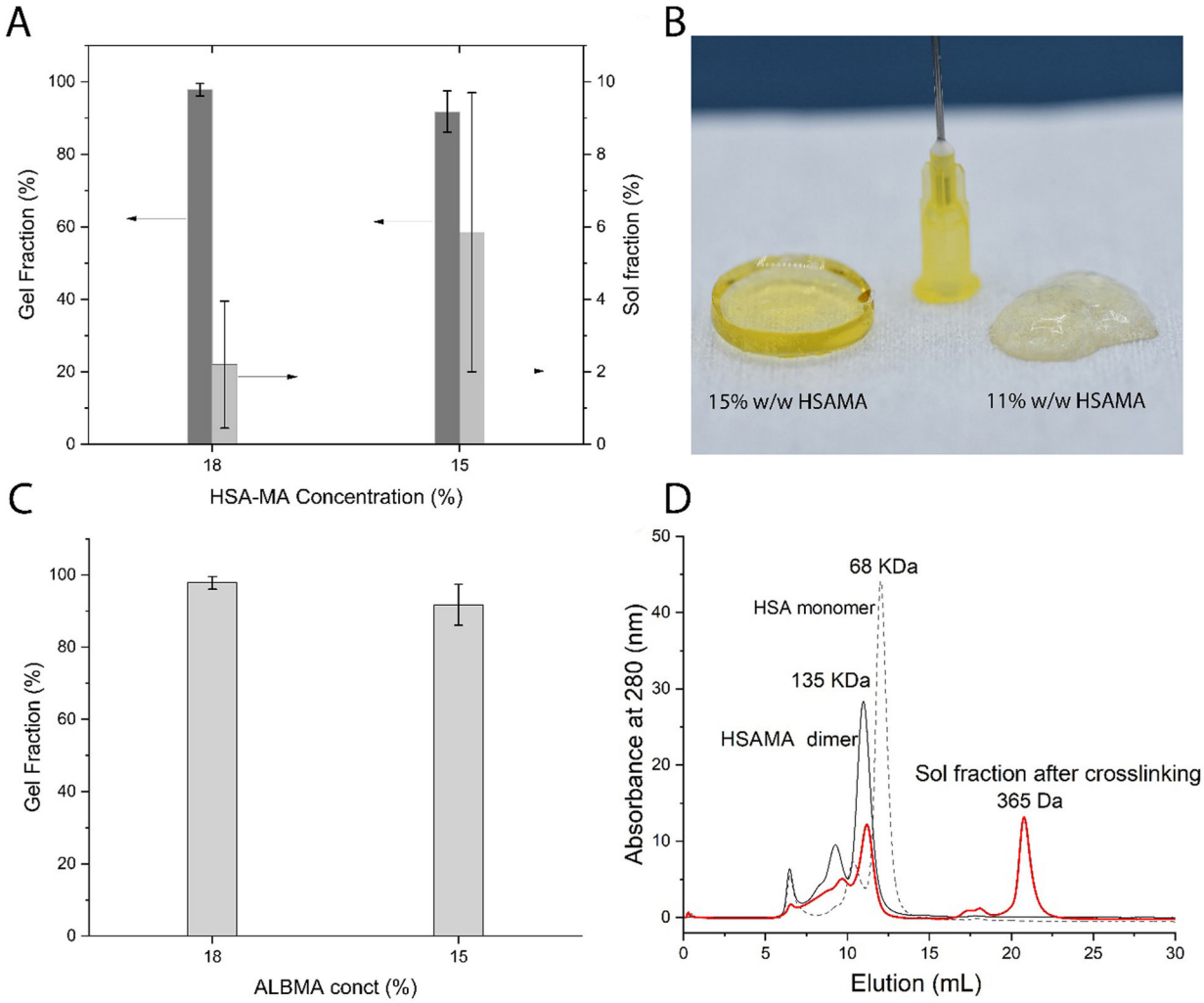

Figure 4.

A, C) The swelling behavior of the HSAMA hydrogel at two different concentrations of 18 and 15% w/w in water (n=5). B, The prepared hydrogel is shown. Left: The hydrogel made from 11% w/w HSAMA has a soft consistency. Right: The hydrogel made from 15% w/w HSAMA. D) The SEC chromatogram of pure HSA and HSAMA monomer and chromatogram of the sol fraction after extraction of photocrosslinked samples in water is shown in red.

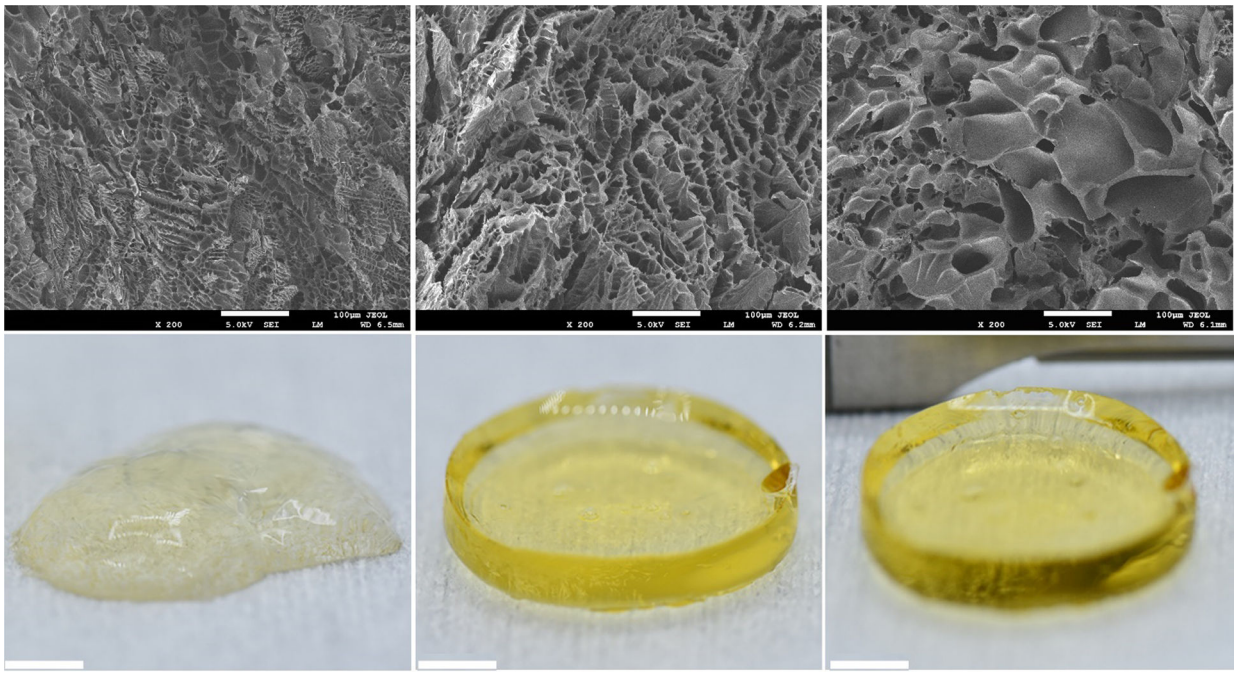

Figure 5.

The microstructure of the HSAMA hydrogels at three different concentrations: 11, 15, and 18 % w/w (from left to right). The synthesized samples were dried using a critical point dryer, and their structure was studied by SEM. The scale bar is 100 micrometers for SEM picture and 2.3 mm for as-prepared hydrogels.

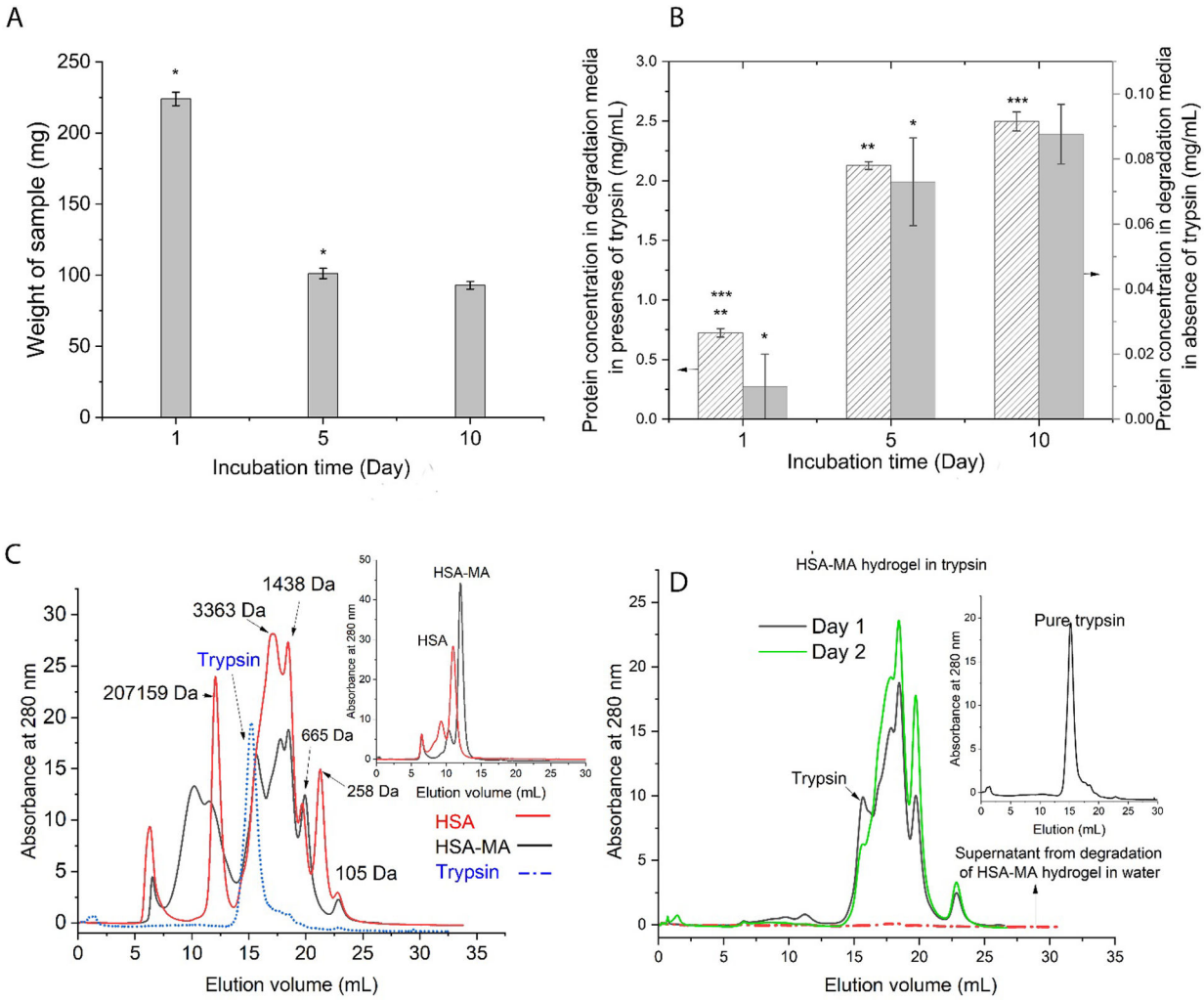

Figure 6.

Analysis of degradation products of HSA, HSAMA, and their hydrogels in both aqueous and enzymatic solution. A) weight reduction of water-swollen albumin hydrogel in enzymatic solution is shown (n=5). Samples were pre-extracted in water to remove the sol fraction before the degradation study. B) The protein content of the degradation medium for study groups in water and the presence of the enzyme are shown within the course of the study (n=3). C) The SEC chromatogram of degradation products of HSA and HSAMA in the presence of trypsin. The insert shows the SEC chromatogram of pure HSA and HSAMA. D) The SEC chromatogram of the supernatants from degradation medium of hydrogels (crosslinked HSAMA) in the presence and absence of trypsin. There is a statistically significant difference ($p<0.05$) in the groups identified by asterisks.

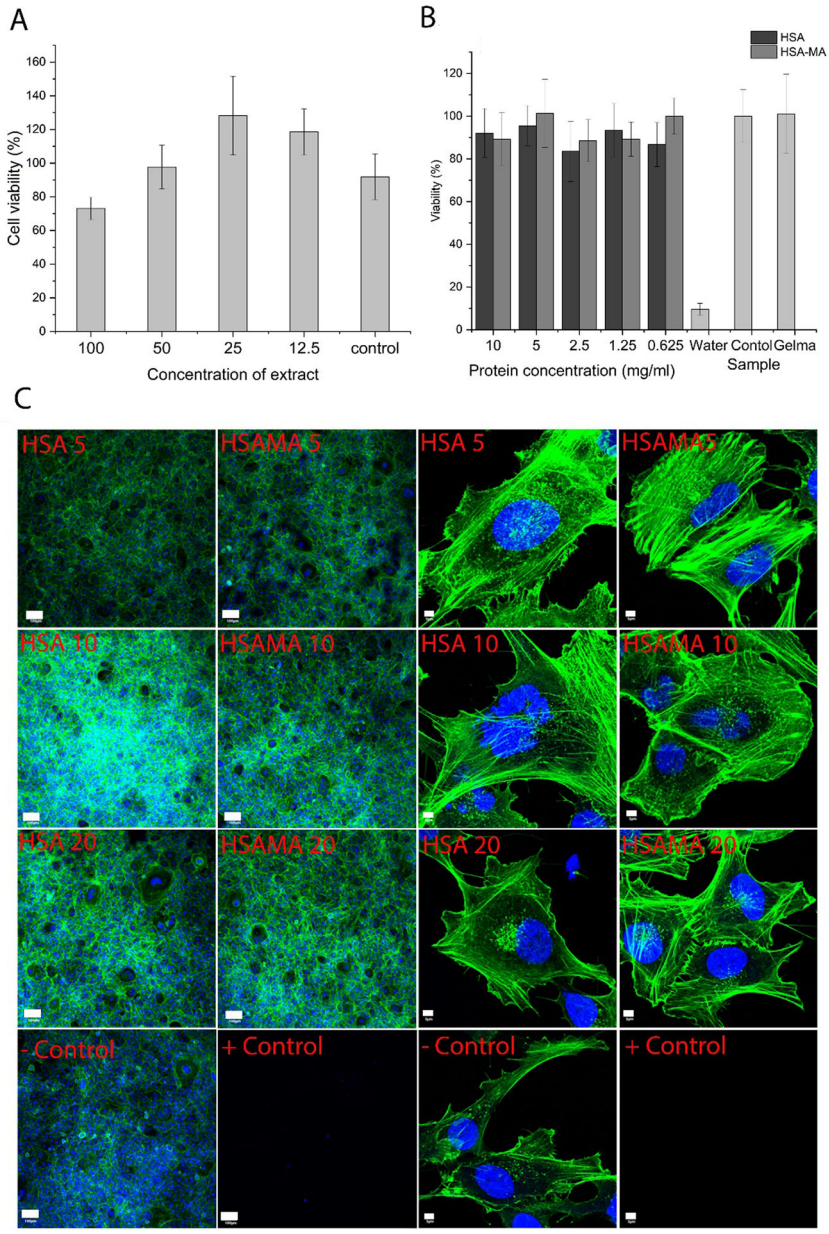

Figure 7.

A, B: Toxicity of the HSA and HSAMA macromers and the corresponding hydrogels as determined by MTT test. A) Following crosslinking, hydrogels were extracted at 0.2 g/mL in complete cell culture medium for 24 h at 37 °C. The preattached HMC3 cells were then treated with the extract in serial dilution with complete cell culture medium. B) The HSA and HSAMA macromers were added at different concentrations to pre-attached HMC3 cells. The toxicity of gelMA macromer at a concentration of 10 mg/mL was also evaluated. C: The morphology of the HMC3 macrophages after treating with HSA and HSAMA macromer at three concentrations of 5, 10, and 20 mg/mL for 24 h was assessed by confocal laser microscopy. The initial cell density of 2×10^4 cell/well was used, and images were obtained at 10X and 120X. The actin filaments were stained with Phalloidin-iFluor 488 (green color),

and the nucleus was stained with DAPi (blue). The top three rows show the HMC3 cells treated with both HSA and HSAMA at concentrations of 5, 10, and 20 mg/mL, respectively. For the negative control, cells were only seeded on the chamber slide. For the positive controls, water was added to fully attached cells. Scale bar represents 100 micrometers for the first two pictures in each row. For the next two images in each row, the scale represents 5 micrometers.

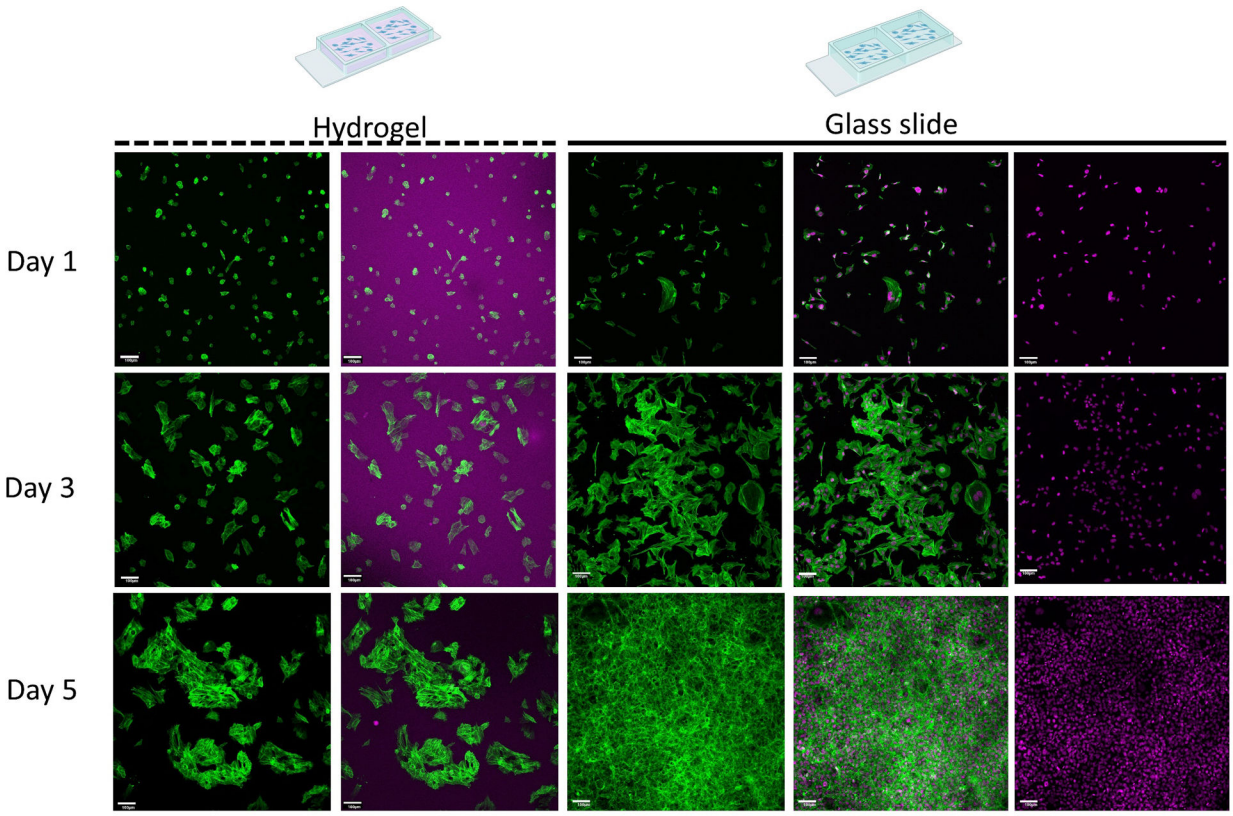

Figure 8.

Morphology of HMC3 cells grown on the surface of albumin hydrogels as well as glass slides after 1-, 3- and 5-day culture as revealed by confocal microscope. The actin filament of the HMC3 cells was stained with Phalloidin-iFluor 488 (shown in green), and the nucleus was stained with Nuc650, a fluorescent DNA nuclear stain (shown in pink). The albumin hydrogels absorbed Nuc65, and the nucleus on the surface of the hydrogel could not be detected. The right two pictures in each row (Day 1, 3, and 5) show the cells on the hydrogels. The left three pictures in each row show the actin filament, the merger of the actin filament and nucleus, and only the nucleus, respectively. The scale bars represent 100 micrometers.

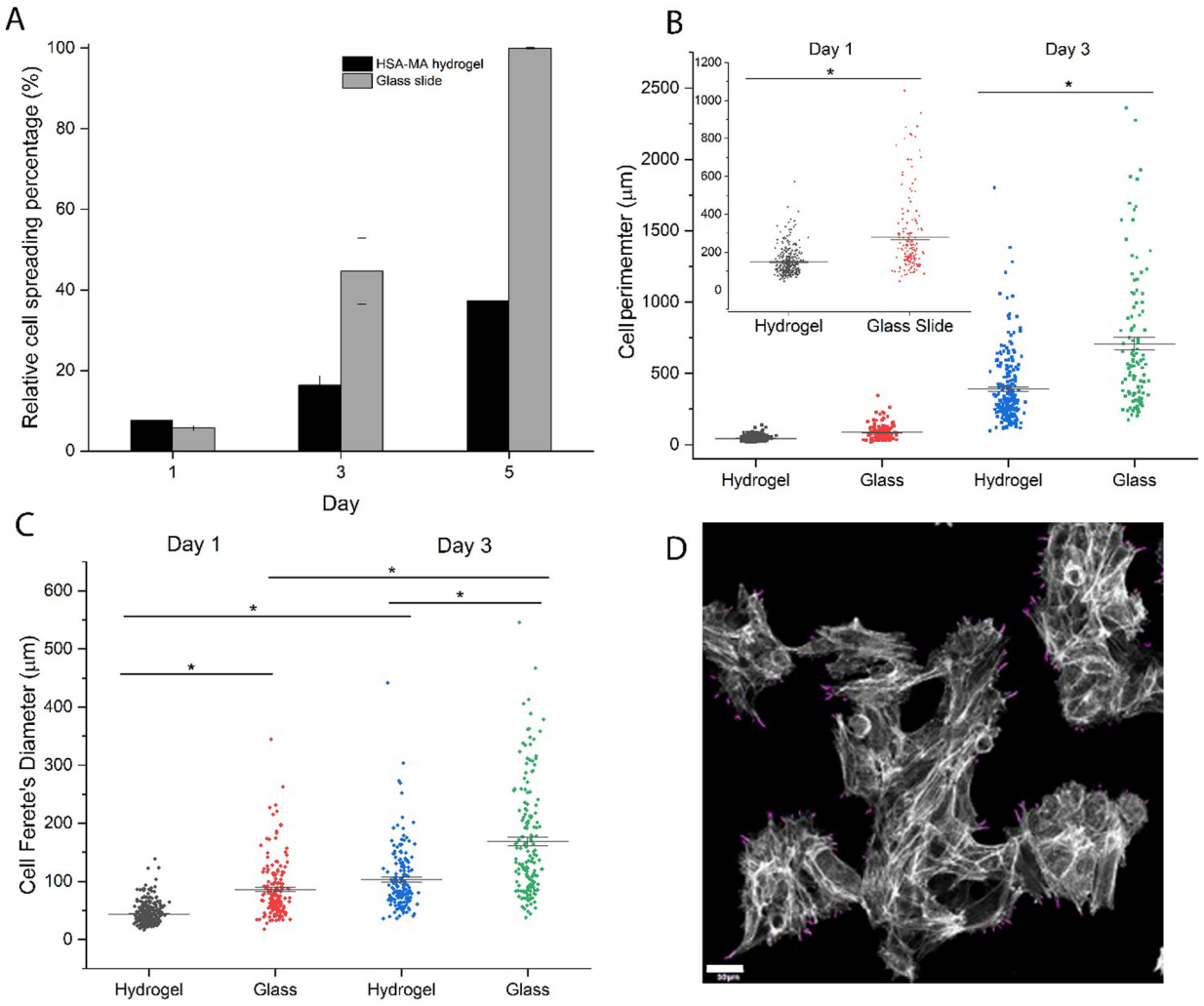

Figure 9.

Cell morphology analysis for HMC3 cells grown on the surface of the albumin hydrogel. (A) The relative spreading area of the cells on the surface of the hydrogels and glass slide after 1, 3, and 5 days' culture. (B) The average perimeter of the HMC3 cells after 1, 3, and 5 days' culture on the surface of albumin hydrogels (C) Average Feret's diameter of HMC3 cells cultured on the hydrogel and glass slides. The image was analyzed by Fiji ImageJ. (D) Filopodia filament visualization on albumin hydrogels on day 5. Visualization was conducted using FilaQuant, FIJI. The value represents mean ± standard deviation for HMC3 cells of ($165<n<306$) for each class. There was a statistically significance difference ($p<0.05$) for the groups identified by asterisks.

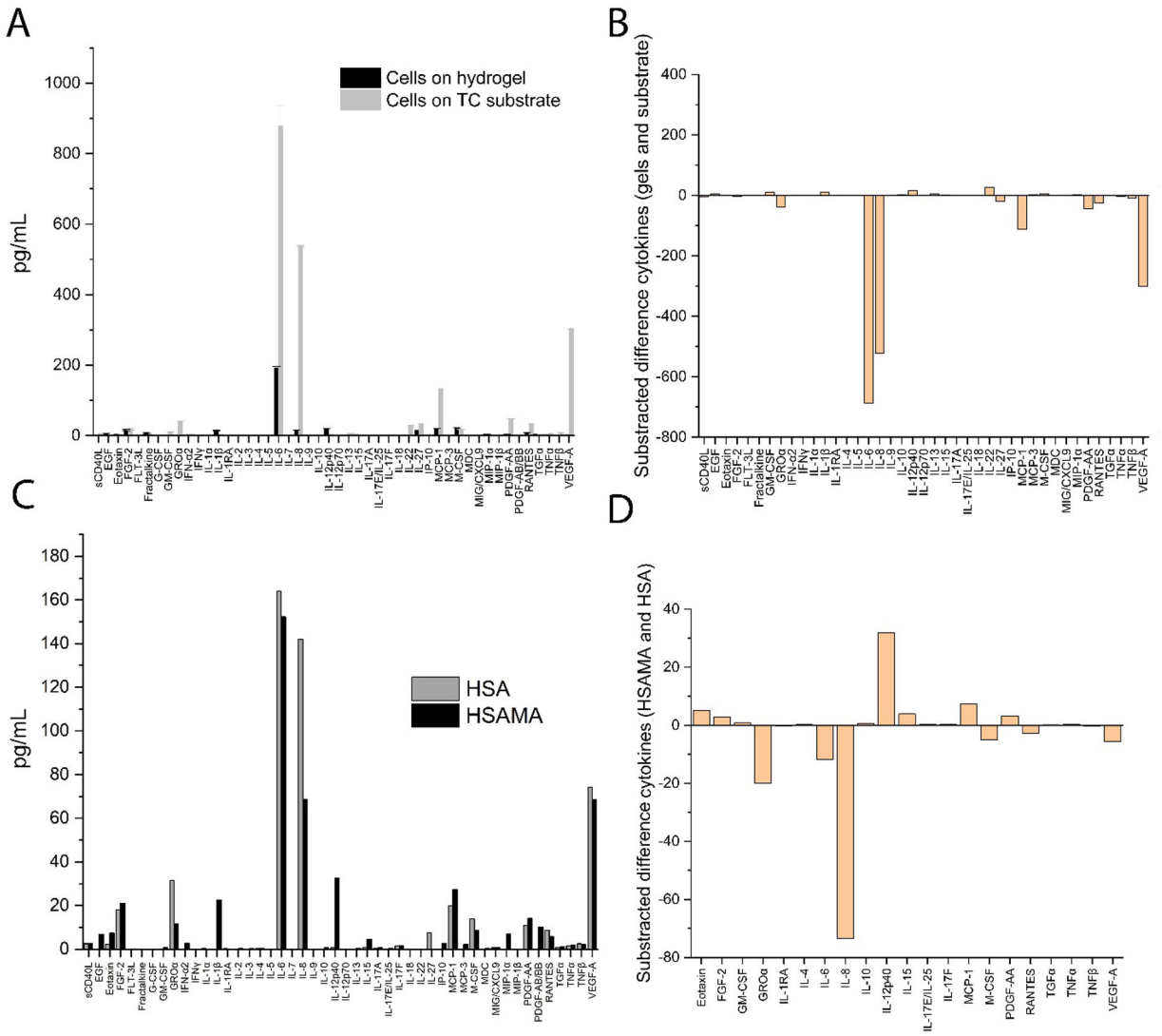

Figure 10.

The inflammatory response of the HMC3 macrophages to HSAMA macromer and resulting hydrogels. For each group, the differential amount is shown next to the picture. The cells were cultured for 24 h. A: The amount of 45 cytokines produced in the media of the cells growing on the surface of the hydrogel and control group is shown. The concentration of IL6 and IL8 is clearly reduced in the hydrogel groups. B: The diffrential cytokins amount between the cells grown on TC and cells on the hydrogels C:The amount of 45 cytokines produced in the culture medium after the addition of 5mg/mL of HSA and HSAMA. D The diffrential cytokins amount between the cells grown in presnese of HAS and HSAMA TC: Tissue culture

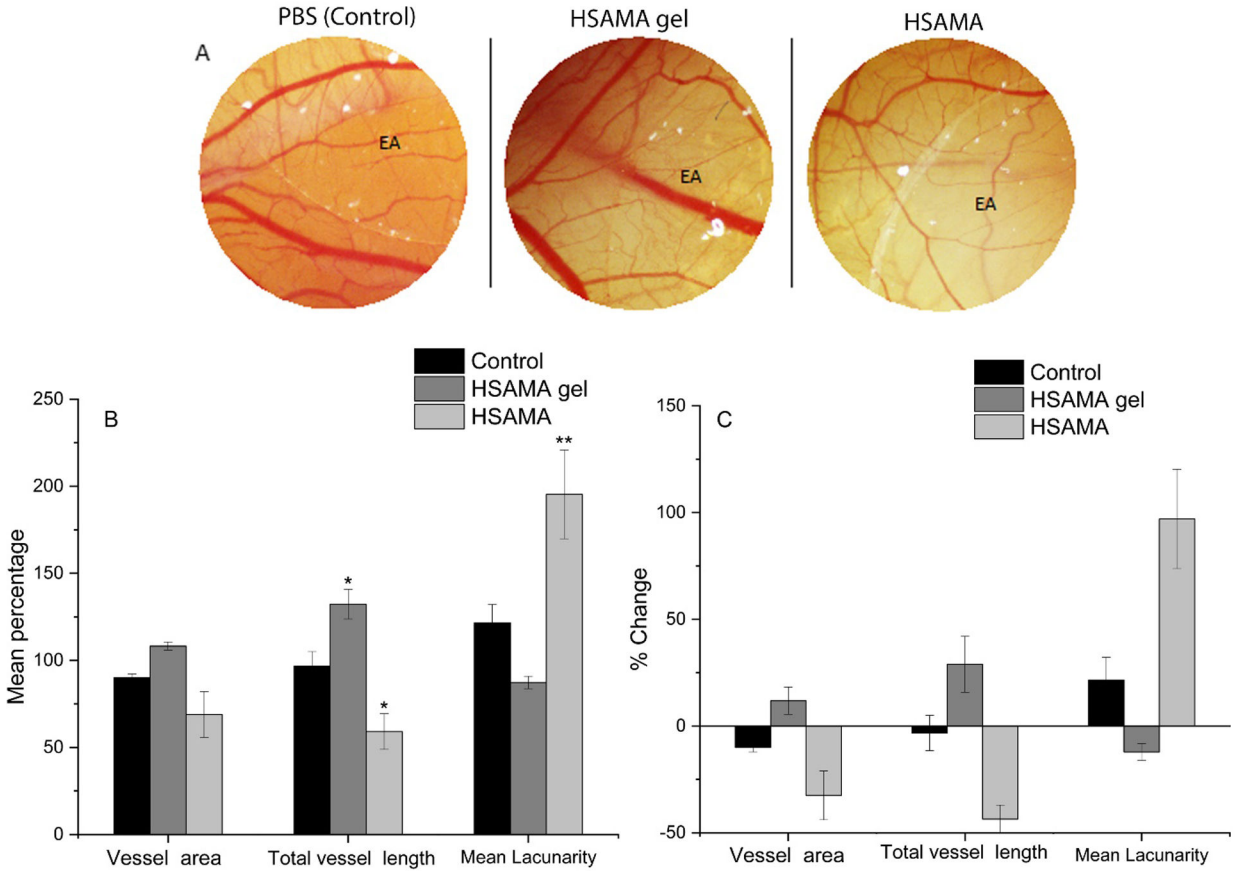

Figure 11.

A: Microscopic images of CAM treated with PBS, HSAMA gel, and HSAMA solution. B: Percentage of the vessels' area, total vessel length, and mean lacunarity. C: Percentage changes of the angiogenesis parameters. Data are represented as mean ± SD, $p^* < 0.05$. Magnification: 20X. EA: EA: exposed area.

Table 1.

Sequence coverage for the unmodified HSA and two different methacrylated batches (M9 and M10) obtained from trypsin and GluC digests.

	Trypsin			GluC		
Search parameter	**Unmodified HSA**	**M9**	**M10**	**Unmodified HSA**	**M9**	**M10**
No modification	92.45%	50.08%	48.44%	91.95%	41.71%	40.56%
Methylacrylate on K	92.45%	84.07%	84.46%	91.95%	89.33%	85.39%
Methylacrylate on CKSTY	92.45%	84.07%	80.46%	91.95%	89.98%	86.54%

Table 2.

The number of modifications with high confidence (>99%) in different HSA samples. Two batches of HSAMA were synthesized using identical formulations and conditions, called M9 and M10, respectively.

Sites	M10-GluC	M9-GluC	M10-trypsin	M10-GluC
Lys	30	47	33	42
Lys, Cys, Thr, Ser, Tyr	56	70	62	61